16aS32-7

ISS搭載CALETによる8年間の観測成果と今後の展望

CALET

Calorimetric
Electron
Telescope

on the International Space Station

鳥居祥二
早稲田大学理工総研
他CALET国際研究チーム

日本物理学会第78回年次大会（東北大学） 2023年9月16日

The CALET Collaboration Member

O. Adriani,[1,2] Y. Akaike,[3,4] K. Asano,[5] Y. Asaoka,[5] E. Berti,[2,13] G. Bigongiari,[6,7] W.R. Binns,[8] M. Bongi,[1,2] P. Brogi,[6,7] A. Bruno,[9] N. Cannady,[10,11,12] G. Castellini,[13] C. Checchia,[6,7] M.L. Cherry,[14] G. Collazuol,[15,16] G.A. de Nolfo,[9] K. Ebisawa,[17] A. W. Ficklin,[14] H. Fuke,[17] S. Gonzi,[1,2,13] T.G. Guzik,[14] T. Hams,[10] K. Hibino,[18] M. Ichimura,[19] K. Ioka,[20] W. Ishizaki,[5] M.H. Israel,[8] K. Kasahara,[21] J. Kataoka,[22] R. Kataoka,[23] Y. Katayose,[24] C. Kato,[25] N. Kawanaka,[20] Y. Kawakubo,[14] K. Kobayashi,[3,4] K. Kohri,[26] H.S. Krawczynski,[8] J.F. Krizmanic,[11] P. Maestro,[6,7] P.S. Marrocchesi,[6,7] A.M. Messineo,[7,27] J.W. Mitchell,[11] S. Miyake,[28] A.A. Moiseev,[11,12,29] M. Mori,[30] N. Mori,[2] H.M. Motz,[31] K. Munakata,[25] S. Nakahira,[17] J. Nishimura,[17] S. Okuno,[18] J.F. Ormes,[32] S. Ozawa,[33] L. Pacini,[2,13] P. Papini,[2] B.F. Rauch,[8] S.B. Ricciarini,[2,13] K. Sakai,[10,11,12] T. Sakamoto,[34] M. Sasaki,[11,12,29] Y. Shimizu,[18] A. Shiomi,[35] P. Spillantini,[1] F. Stolzi,[6,7] S. Sugita,[34] A. Sulaj,[6,7] M. Takita,[5] T. Tamura,[18] T. Terasawa,[5] S. Torii,[3] Y. Tsunesada,[36,37] Y. Uchihori,[38] E. Vannuccini,[2] J.P. Wefel,[14] K. Yamaoka,[39] S. Yanagita,[40] A. Yoshida,[33] K. Yoshida,[21] and W. V. Zober[8]

PI : Japan Co-PI : Italy Co-PI : USA

1) University of Florence, Italy
2) INFN Florence, Italy
3) WISE, Waseda University, Japan
4) JEM Utilization Center, JAXA, Japan
5) ICRR, University of Tokyo, Japan
6) University of Siena, Italy
7) INFN Pisa, Italy
8) Washington University, St. Louis, USA
9) Heliospheric Physics Laboratory, NASA/GSFC, USA
10) University of Maryland, Baltimore County, USA
11) Astroparticle Physics Laboratory, NASA/GSFC, USA
12) CRESST, NASA/GSFC, USA
13) IFAC, CNR, Italy
14) Louisiana State University, USA
15) University of Padova, Italy
16) INFN Padova, Italy
17) ISAS, JAXA, Japan
18) Kanagawa University, Japan
19) Hirosaki University, Japan
20) YITP, Kyoto University, Japan
21) Shibaura Institute of Technology, Japan
22) ASE, Waseda University, Japan
23) NIPR, Japan
24) Yokohama National University, Japan
25) Shinshu University, Japan
26) IPNS, KEK, Japan
27) University of Pisa
28) NIT(KOSEN), Ibaraki College, Japan
29) University of Maryland, College Park, USA
30) Ritsumeikan University, Japan
31) GCSE, Waseda University, Japan
32) University of Denver, USA
33) NICT, Japan
34) Aoyama Gakuin University, Japan
35) Nihon University, Japan
36) Osaka Metropolitan University, Japan
37) NITEP, Osaka Metropolitan University, Japan
38) QST, Japan
39) Nagoya University, Japan
40) Ibaraki University, Japan

Guest Investigator: Lauren W. Blum (University of Colorado Boulder, USA), M. Teramoto (Kyushu Institute of Technology, Japan)

CALET Payload

Kounotori (HTV) 5

Launched on Aug. 19th, 2015 by the Japanese H2-B rocket

Emplaced on JEM-EF port #9 on Aug. 25th, 2015

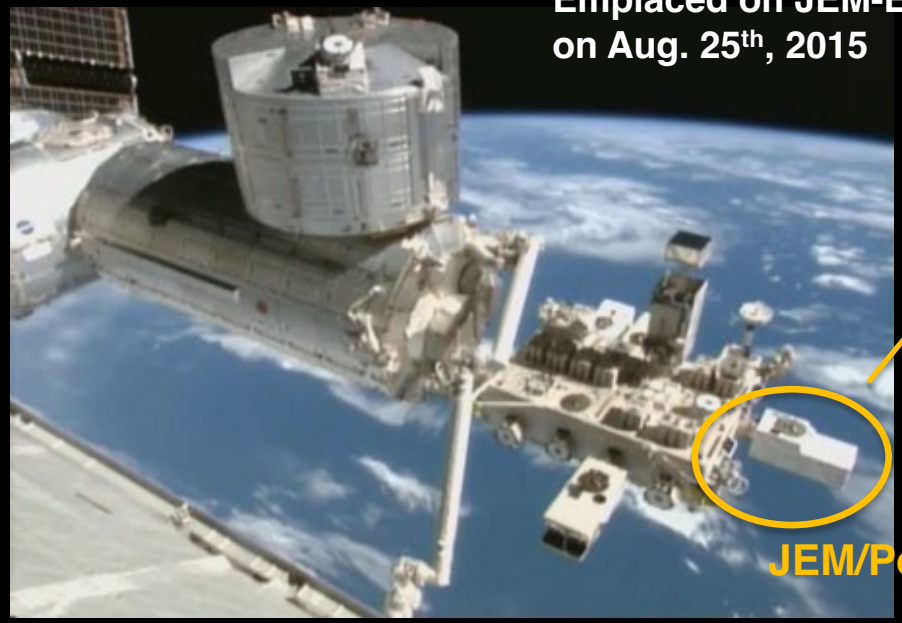

JEM/Port #9

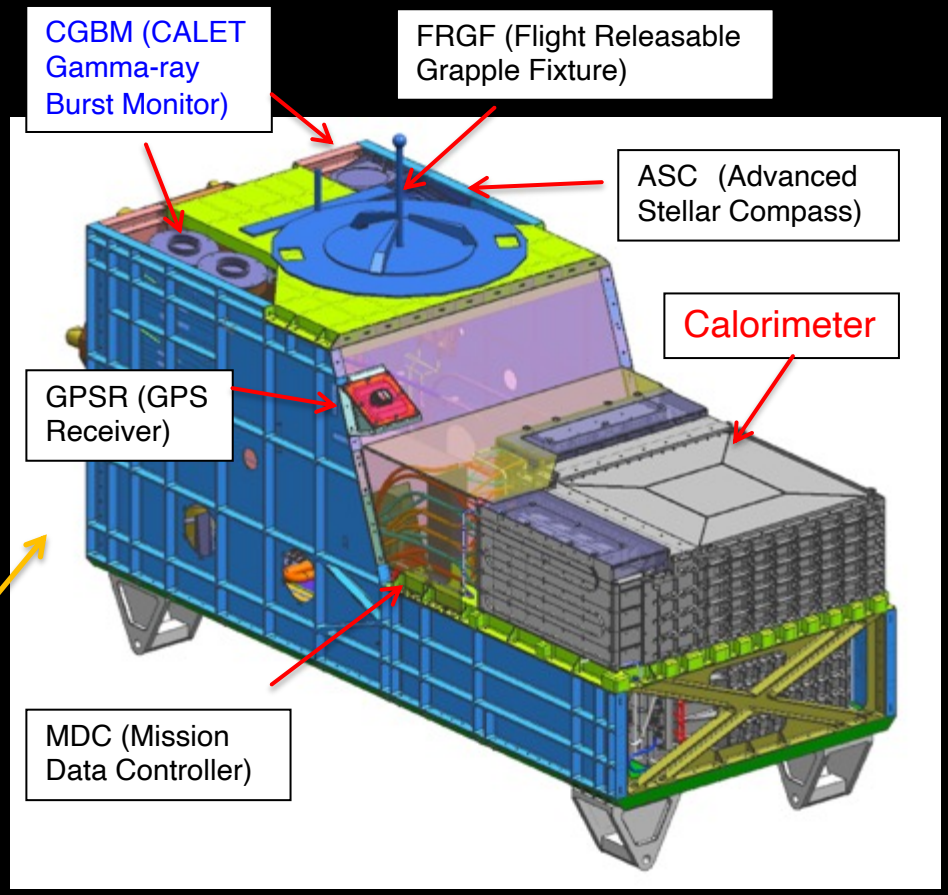

- **Mass: 612.8 kg**
- **JEM Standard Payload Size:**
  1850mm(L) × 800mm(W) × 1000mm(H)
- **Power Consumption: 507 W（max）**
- **Telemetry:**
  Medium 600 kbps (6.5GB/day) / Low 50 kbps

Overview of the CALET Calorimeter

Field of view: ~ 45 degrees (from the zenith) : Geometrical Factor: ~ 1,040 cm^{2}sr (for electrons) : Thickness: 30 X_0, 1.3 λ_I

CHD/IMC

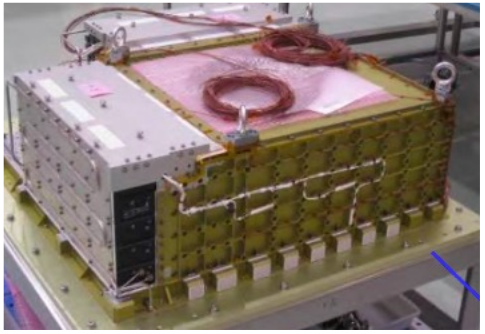

TASC

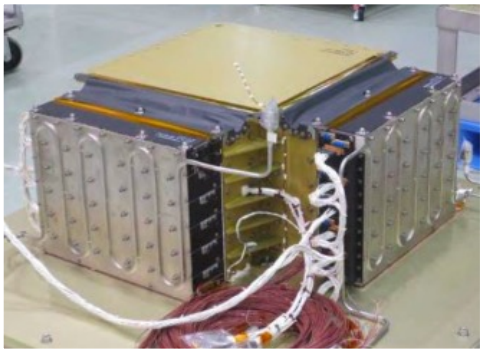

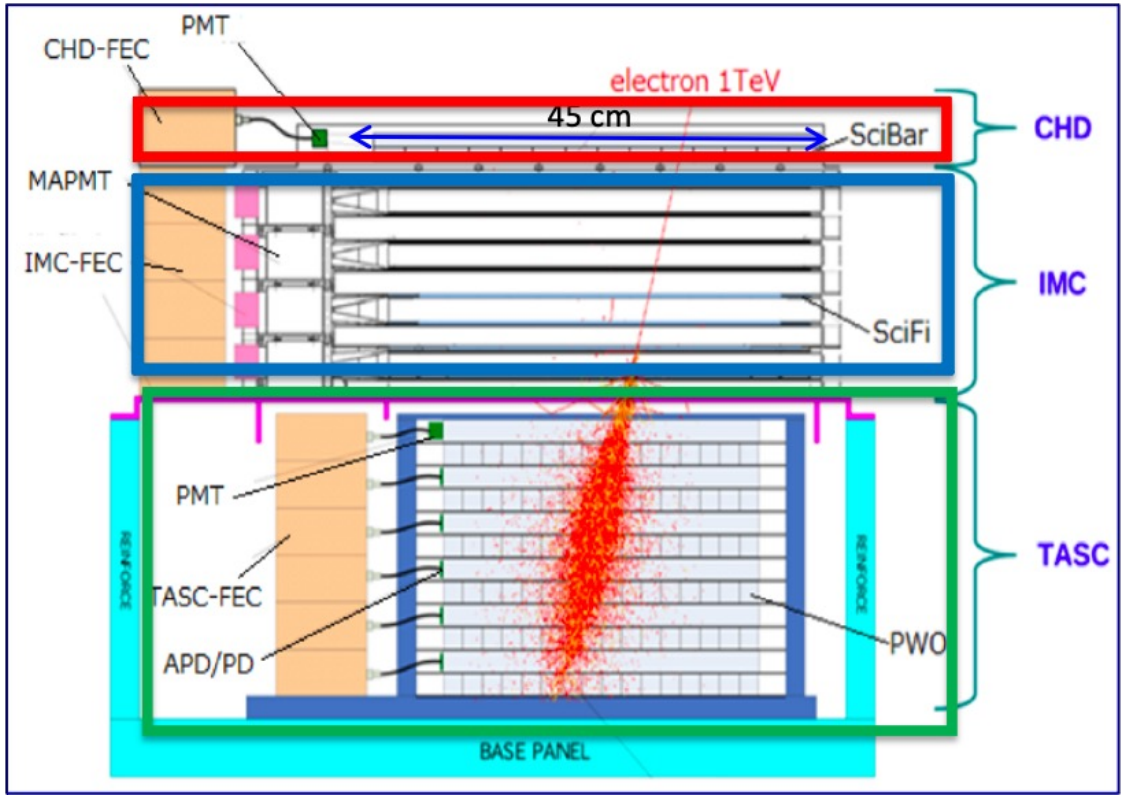

CHD – Charge Detector

- 2 layers x 14 plastic scintillating paddles
- **single element charge ID** from p to Fe and above (Z = 40)
- charge resolution ~0.1-0.3 e

IMC – Imaging Calorimeter

- Scifi. + tungsten absorbers: **3 X_0**
- 8 x 2 x 448 plastic scintillating fibers (1mm) **readout individually**
- **tracking** (~0.1° angular resolution) + **Shower imaging**

TASC – Total Absorption Calorimeter

- 6 x 2 x 16 lead tungstate ($PbWO_4$) logs: **27 X_0, 1.2 λ_I**
- **energy resolution:** ~2 % (>10GeV) for e , γ ~30-35% for p, nuclei
- **e/p separation:** ~10^{-5}
- **angular resolution:** 0.2° for gamma-rays > ~50 GeV

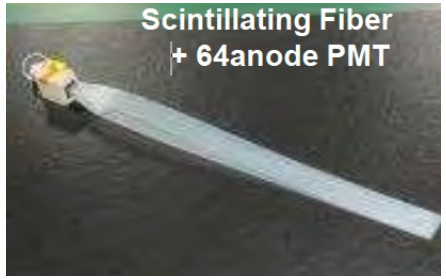

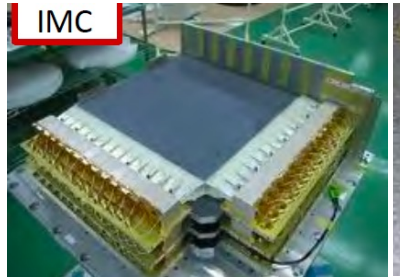

Examples of CALET Event Candidates

Electron, E=3.05 TeV

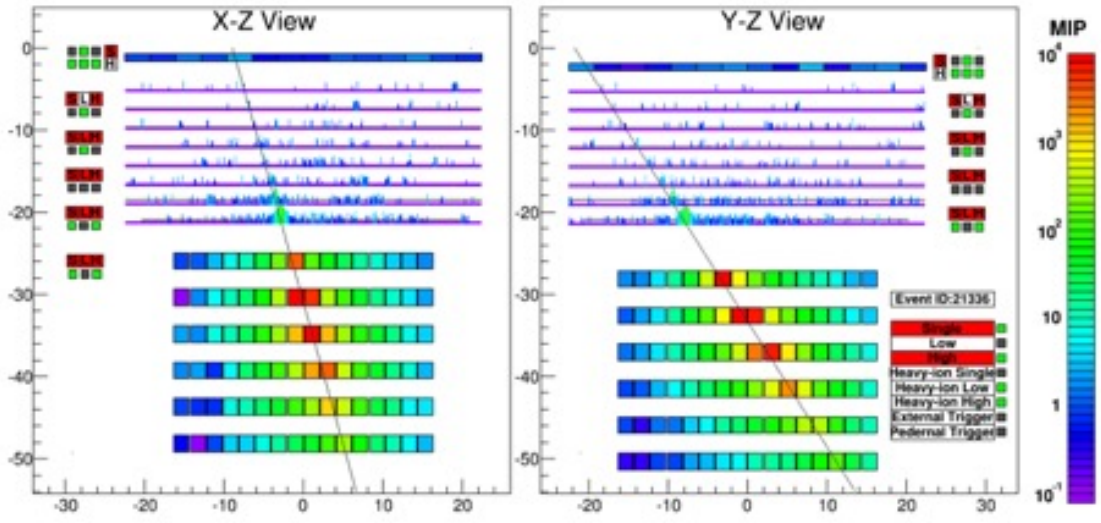

Proton, E_{TASC}=2.89 TeV

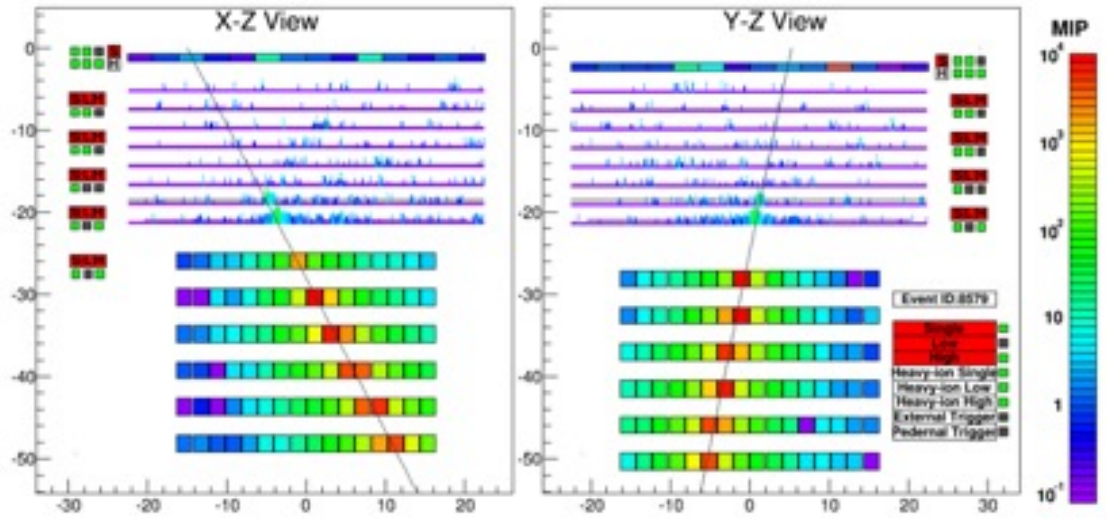

Gamma-ray, E=44.3 GeV

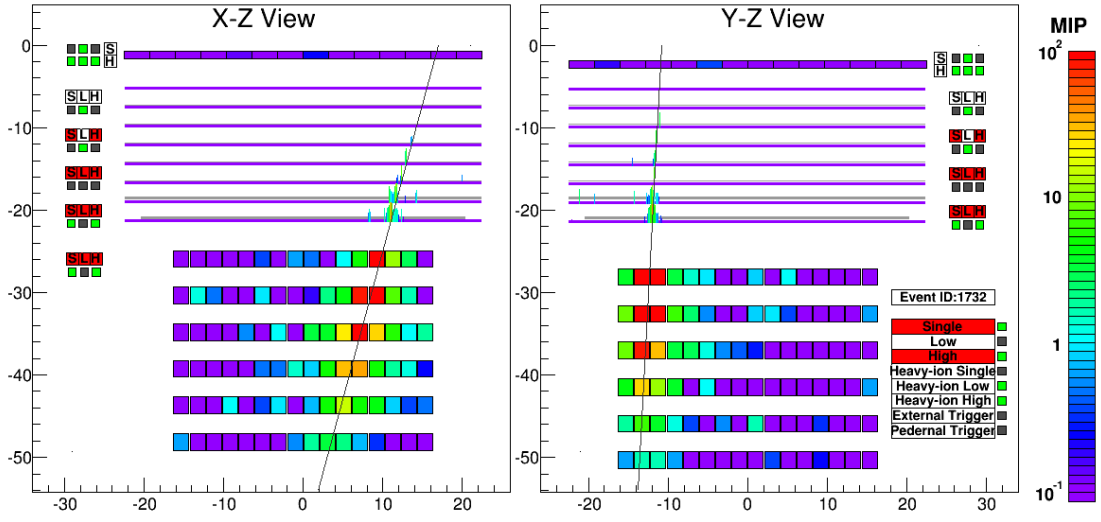

Iron, E_{TASC} =9.3 TeV

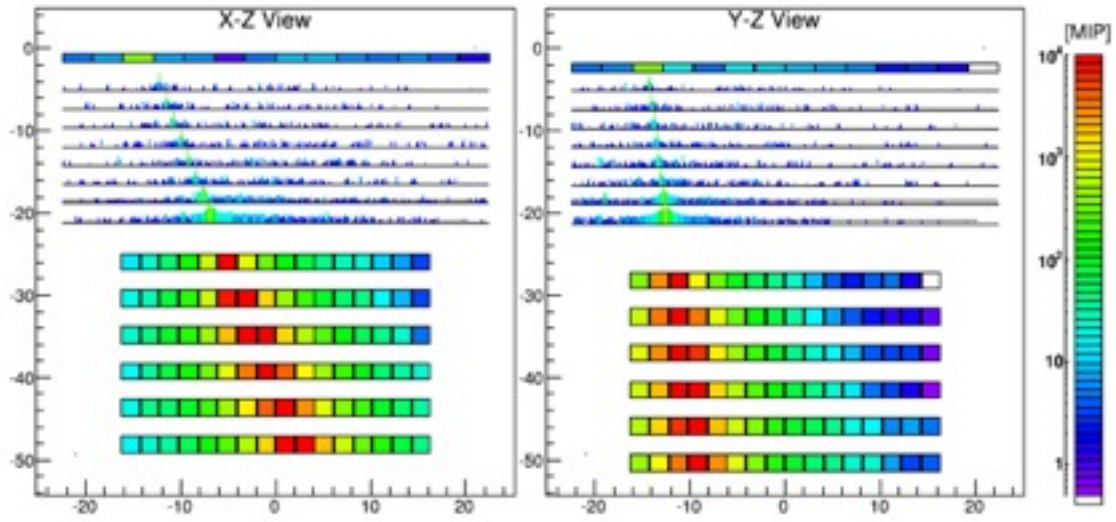

CALET Orbital Operations

Geometrical Factor:
- 1040 cm^2 sr for electrons, light nuclei
- 1000 cm^2 sr for gamma-rays
- 4000 cm^2sr for ultra-heavy nuclei

High-energy trigger (> 10 GeV) statistics:
- Orbital operations : **2818 days (>7.5 years)** as of June 30, 2023
- Observation time : 2.39×10^8 sec
- Live time fraction: ～ **86%**
- Exposure of HE trigger : **～250 m^2 sr day**

Time duration of observation (day by day)

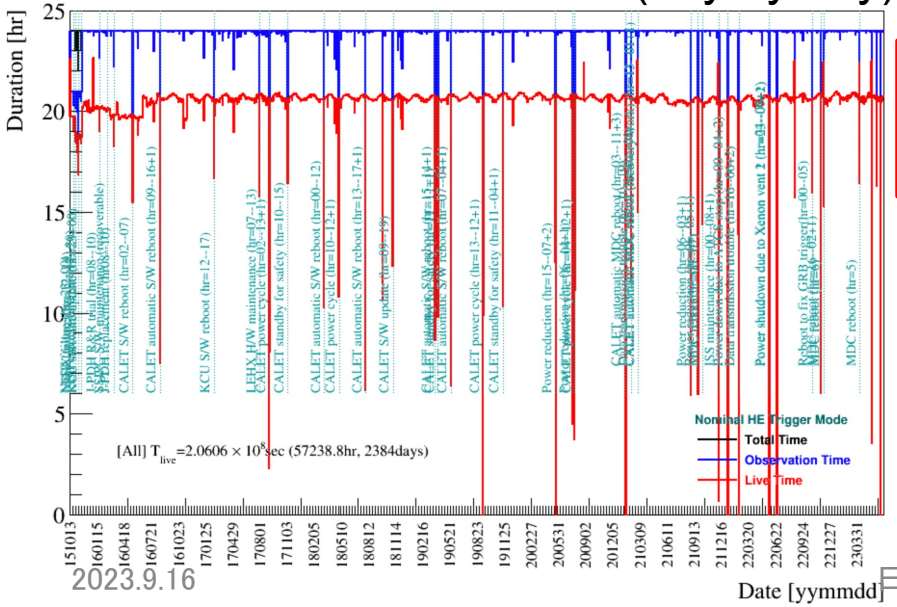

20.6 hours per day on average

Energy deposit (in TASC) spectrum: 1 GeV-1 PeV

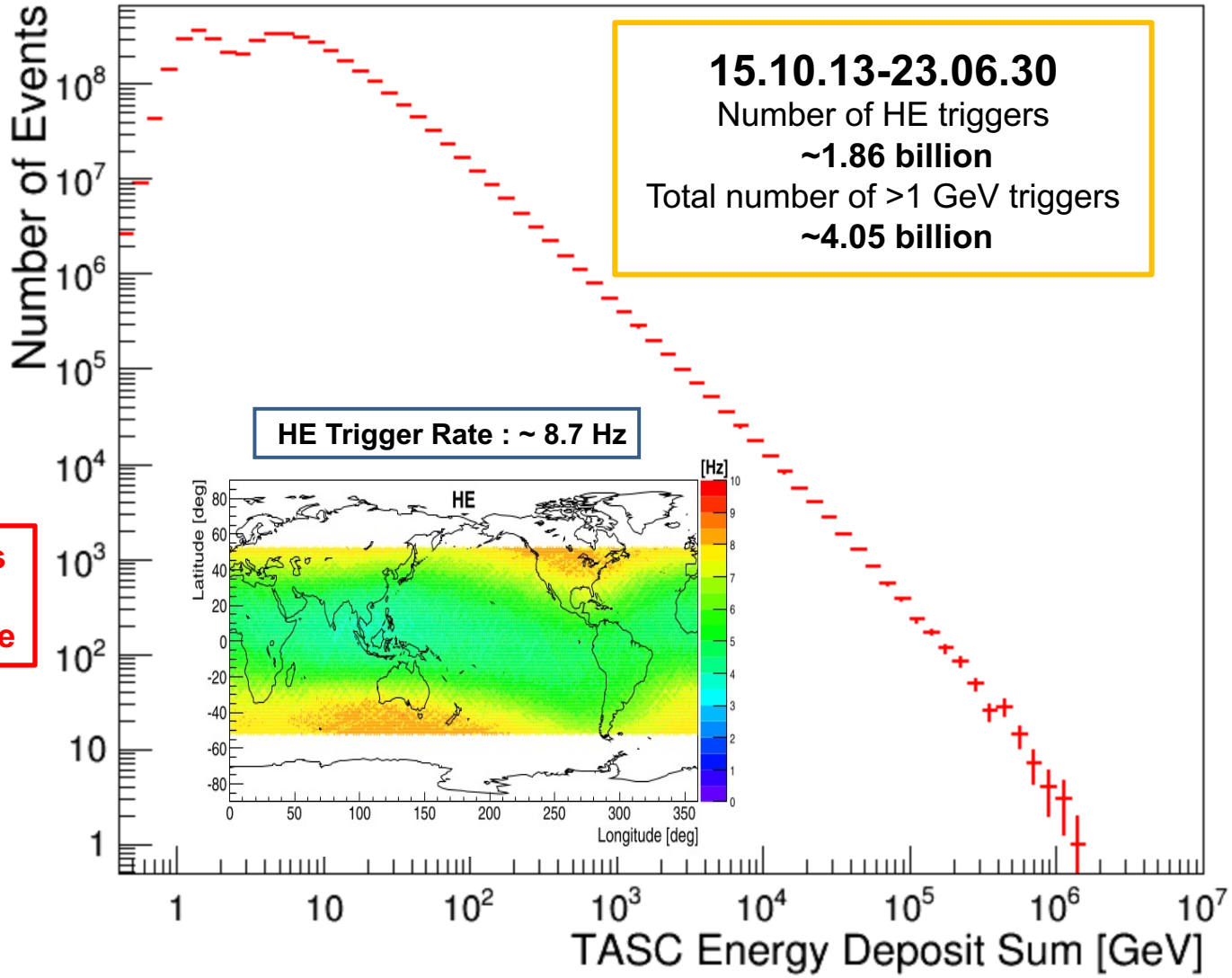

Cosmic-ray All-electron Spectrum up to 7.5 TeV

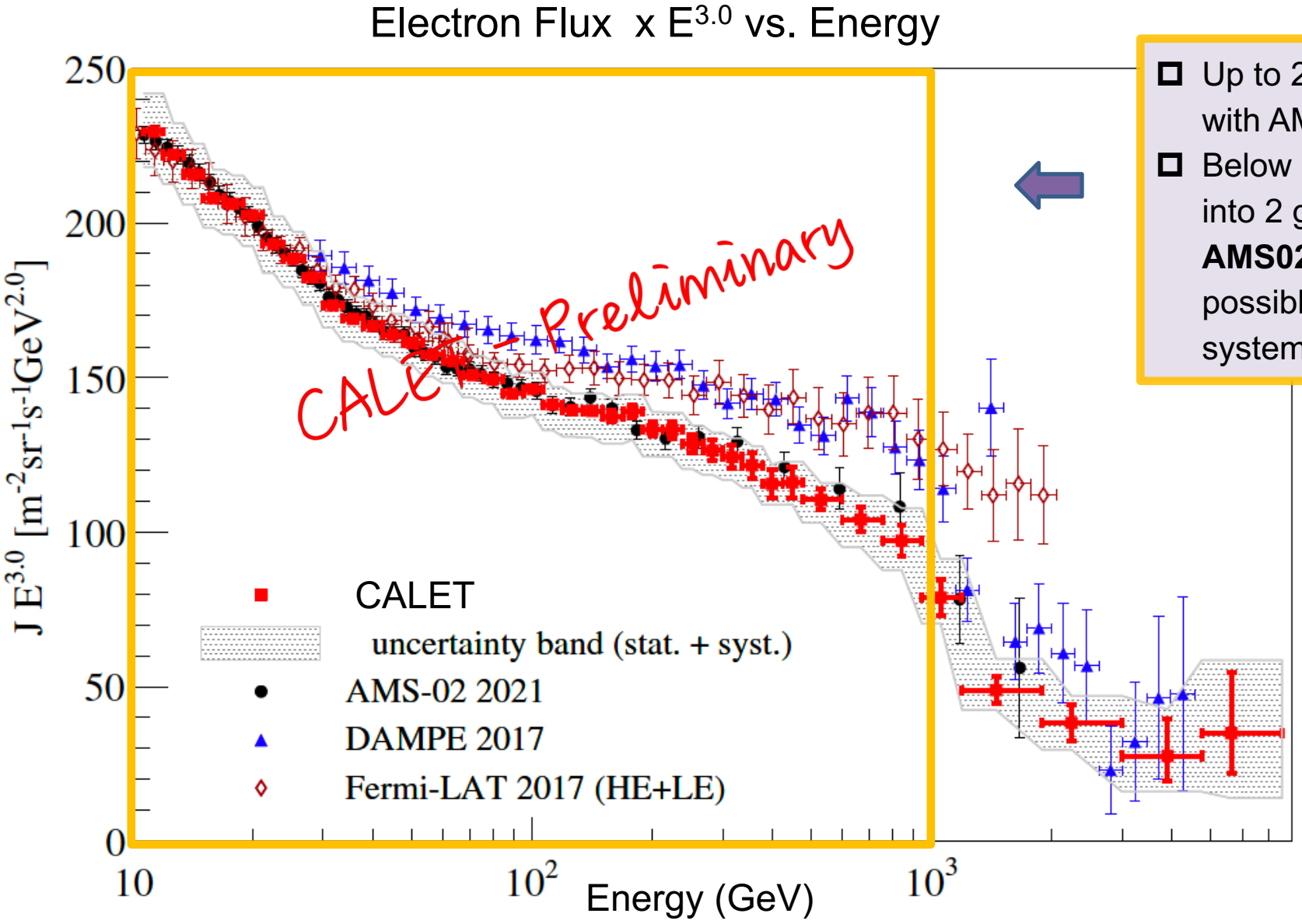

- Up to 2 TeV : CALET spectrum is consistent with AMS-02
- Below 1 TeV : Present measurements cluster into 2 groups:
  AMS02 + CALET and **FERMI + DAMPE**
  possibly indicating the presence of unkown systematics

Preliminary spectrum is **updated** using 2637 days of CALET observations:
Oct.13, 2015 – Dec. 31, 2022
7.02 million events > 10 GeV

Cosmic-ray All-electron Spectrum up to 7.5 TeV

16aS32-8: 赤池陽水

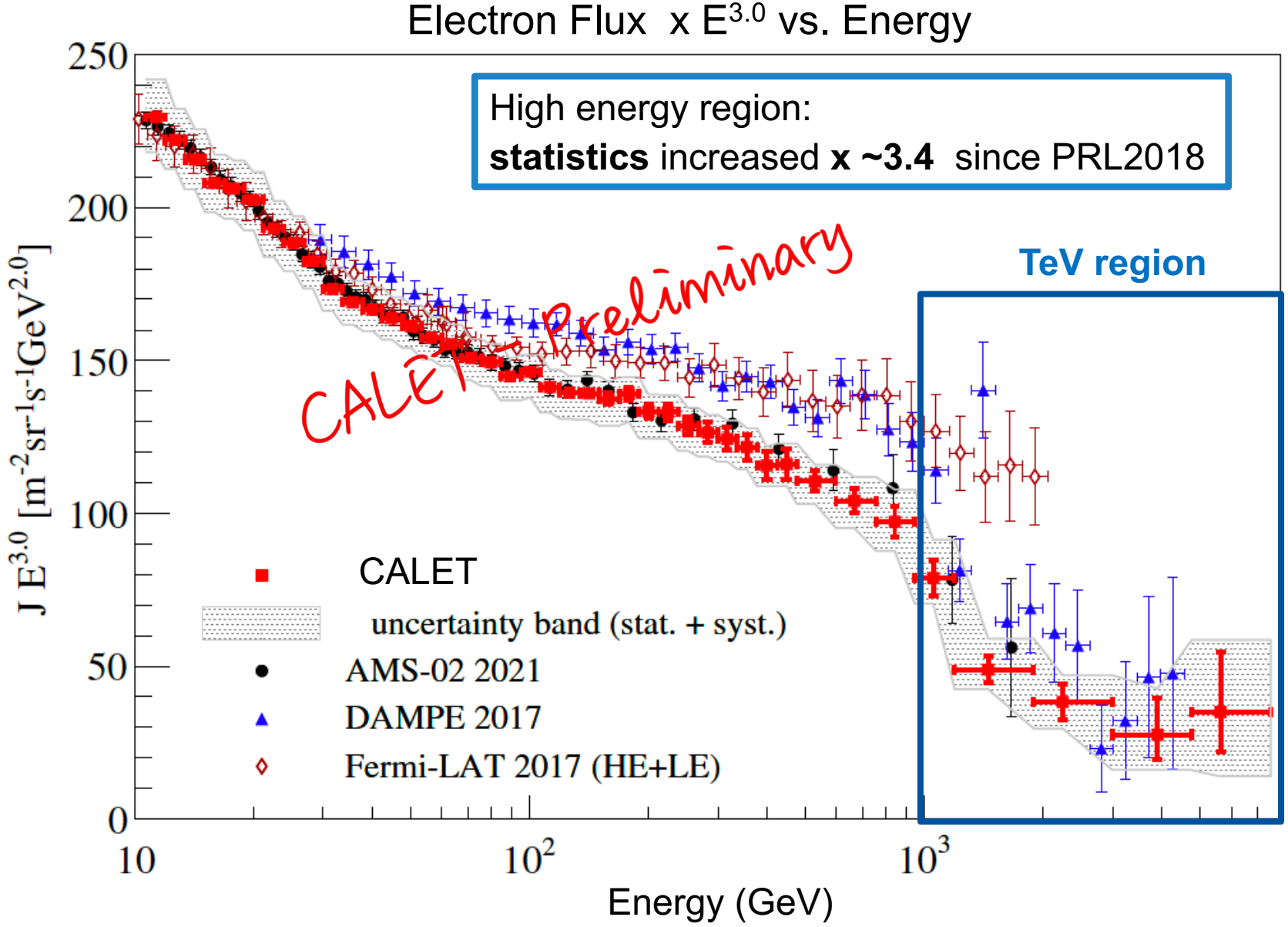

Energy loss due to Synchrotron and Inverse Compton : $dE/dt = -bE^2$

⇨ Observable sources of the electrons in the TeV region should be located at a distance < ~1 kpc and produced at a year < ~10^5 yr.

⇨ **Softening of the spectrum is expected above 1 TeV** since only a few SNRs are observed to keep this condition.

CALET observes a flux suppression above 1 TeV with a **significance > 6 σ**, a considerable improvement with respect to the result published in PRL2018 (~4 σ).

Advanced analysis is going on for electron identification above 5 TeV.

Towards an Interpretation of the CALET All-electron Spectrum

16aS32-12: H.Motz

Tentative spectral fits of the CALET all-electron spectrum in 10 GeV-7.5 TeV including pulsars and a possible Vela SNR contribution:

- The positron flux of AMS-02 is shown with expected contributions (red line) from secondaries (red dashed line) and sum of several pulsars (red dotted line).
- The electron flux is shown with contribution from by secondaries + distant SNRs (black dashed line) and the Vela SNR (green line).
- The fitted model includes a possible contribution from the Vela SNR , consistent with an energy output of 0.7 x 10^{48} erg in electron CR above 1 GeV.

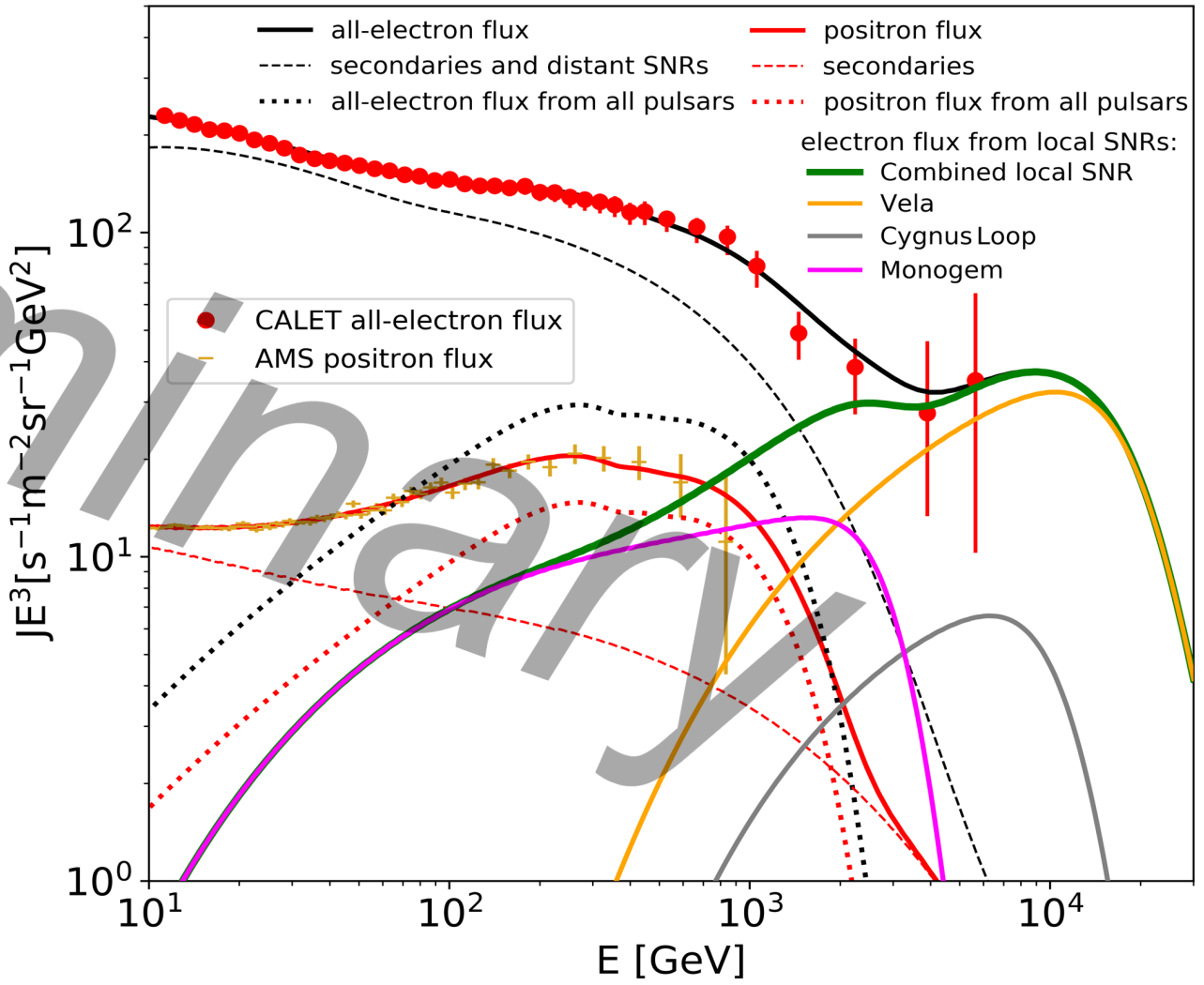

Cosmic-ray Proton Spectrum

16aS32-9: 小林兼好

Flux x $E^{2.7}$ vs. Kinetic energy [Oct.2015- Apr.2023]

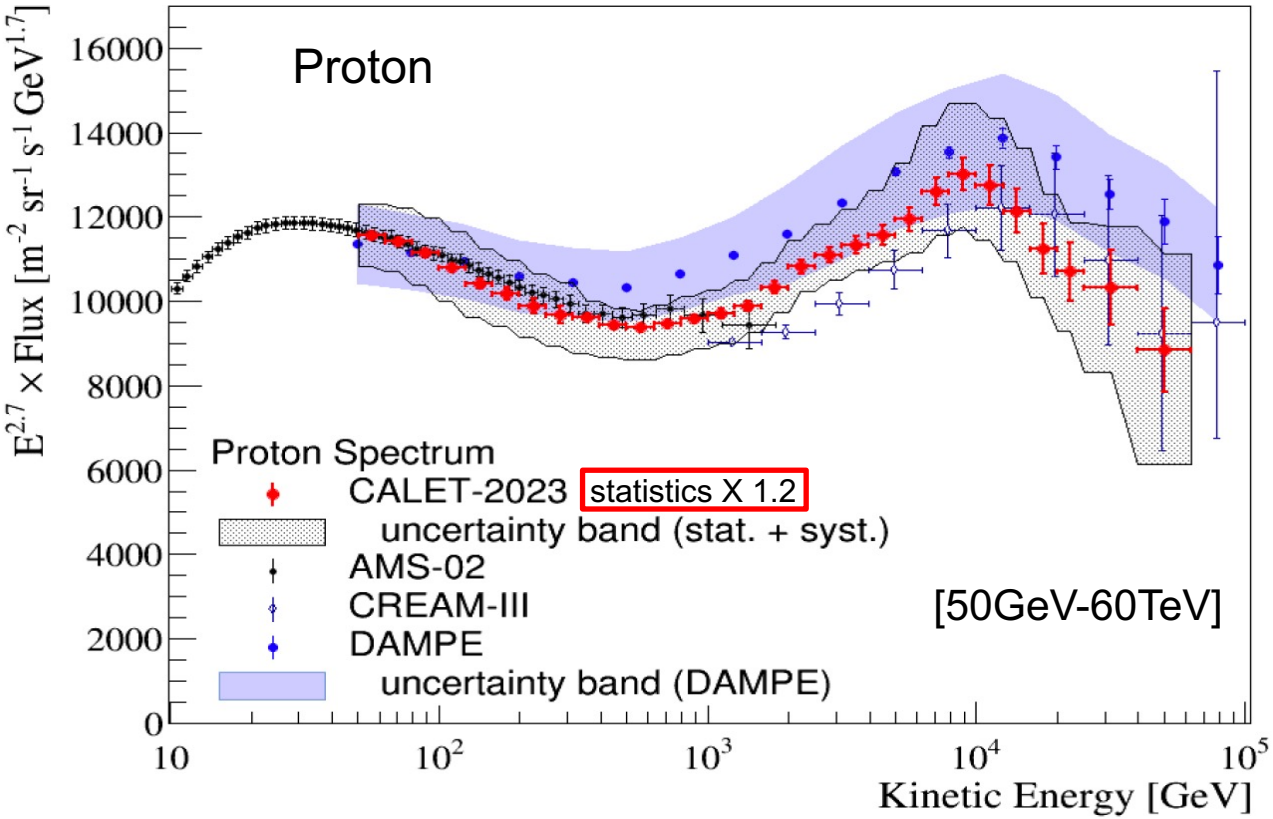

Fitting by DBPL Function

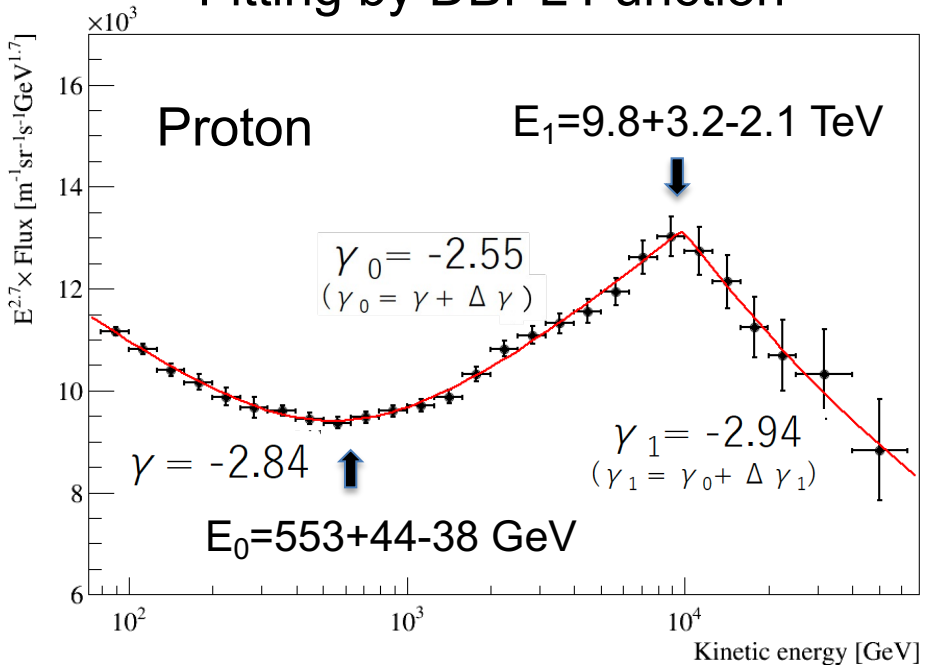

Energy dependence of power index

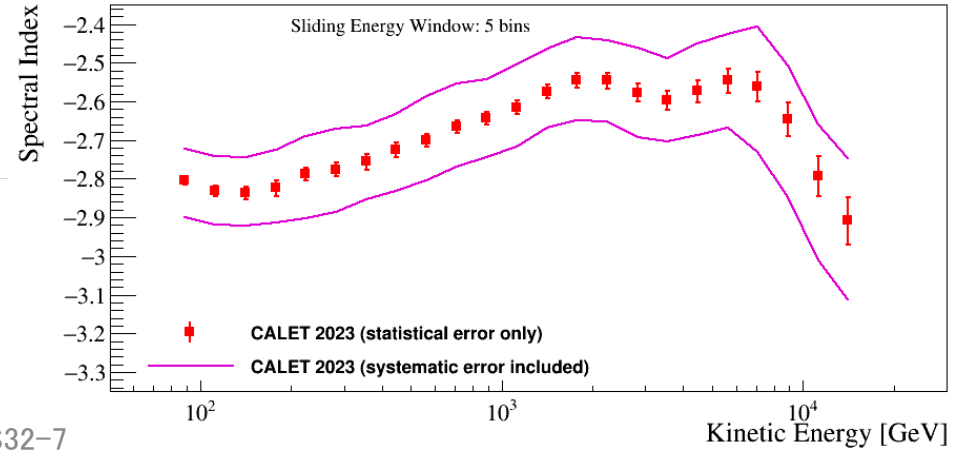

Double Power Law Function: HARDENING SOFTENING

$$\Phi(E) = C \times \left(\frac{E}{1\ \mathrm{GeV}}\right)^{\gamma} \times \left[1 + \left(\frac{E}{E_0}\right)^{s}\right]^{\frac{\Delta\gamma}{s}} \times \left[1 + \left(\frac{E}{E_1}\right)^{s_1}\right]^{\frac{\Delta\gamma_1}{s_1}}$$

Cosmic-ray Helium Spectrum

16aS32-9: 小林兼好

Flux x $E^{2.6}$ vs. Kinetic energy [Oct. 2015 - Apr. 2022]

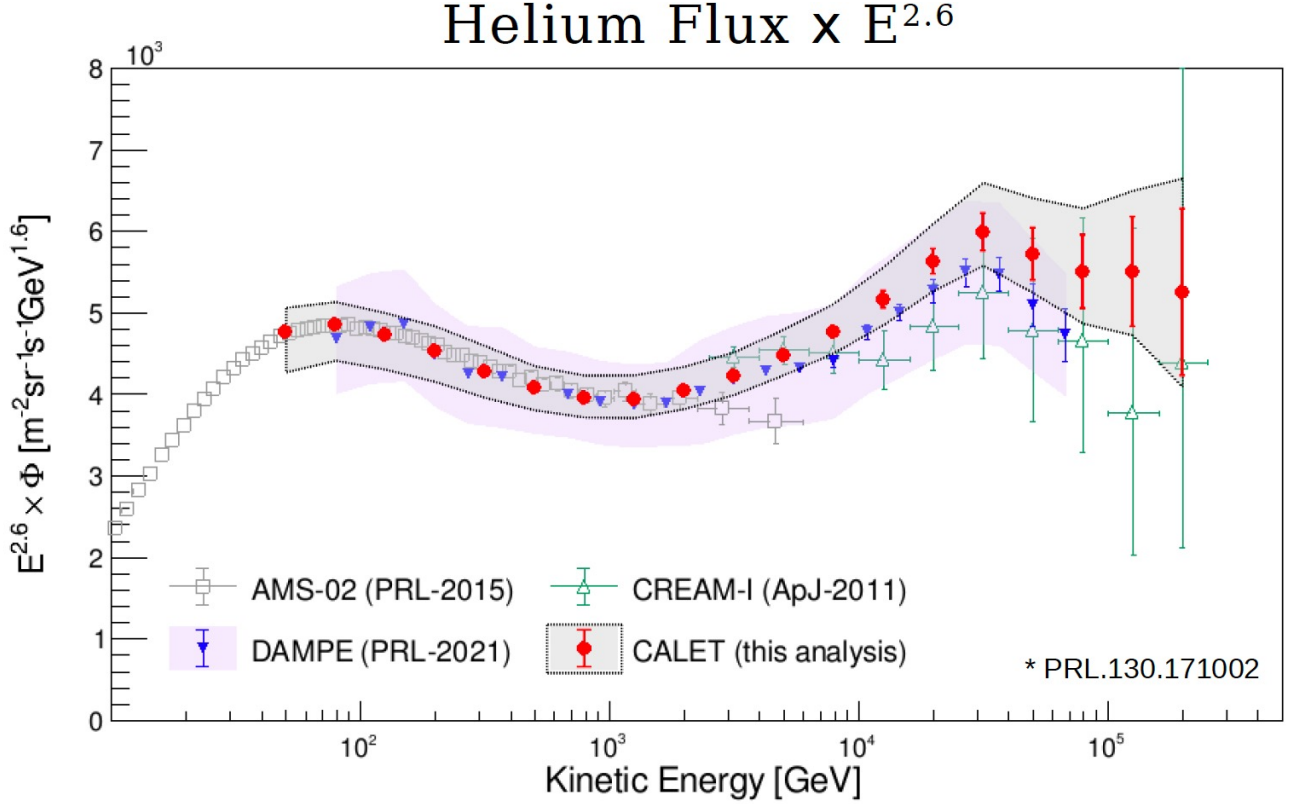

Fitting by Double Power Law (DBPL) function

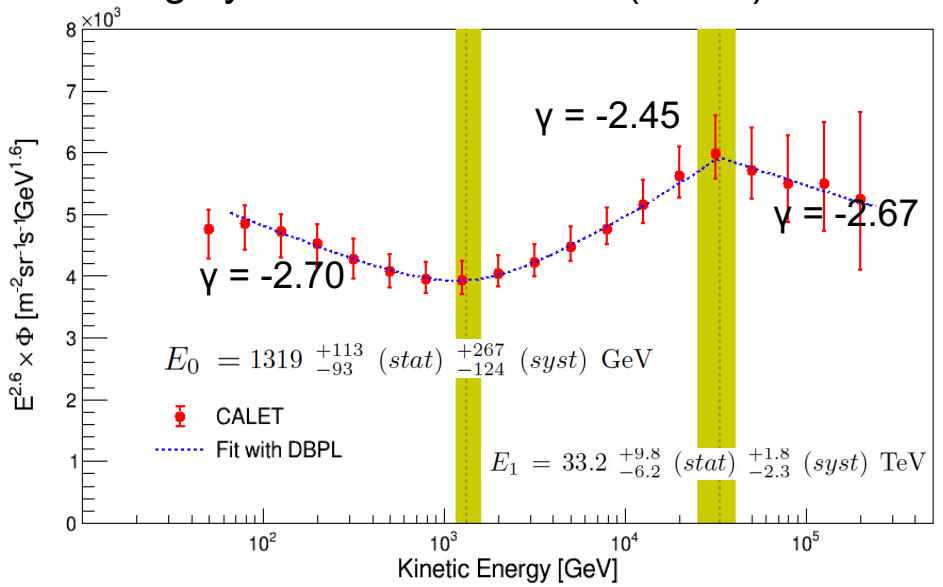

Energy dependence of power index

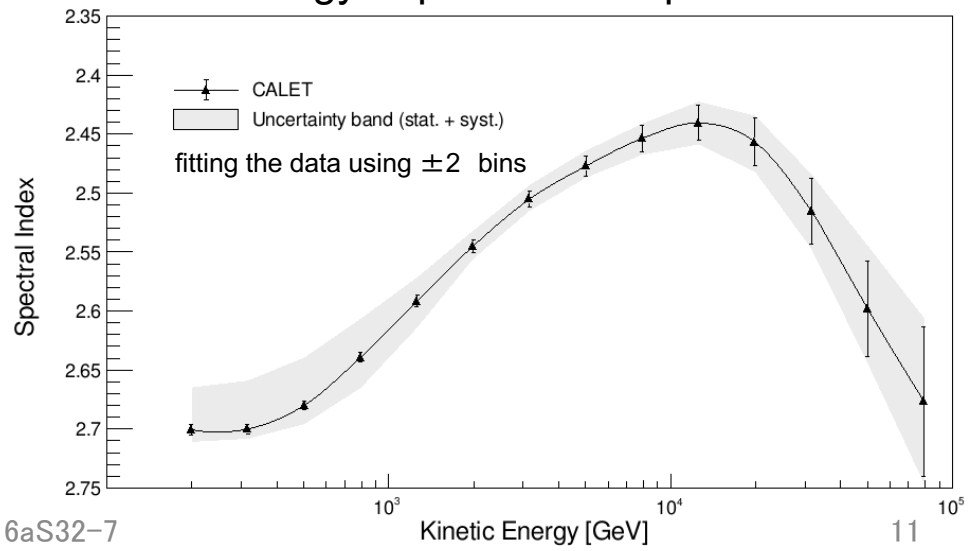

Double Power Law Function: HARDENING SOFTENING

$$\Phi(E) = C\left(\frac{E}{GeV}\right)^{\gamma}\left[1+\left(\frac{E}{E_0}\right)^{S}\right]^{\frac{\Delta\gamma}{S}}\left[1+\left(\frac{E}{E_1}\right)^{S_1}\right]^{\frac{\Delta\gamma_1}{S_1}}$$

Carbon, Oxygen and Boron Energy Spectra

Flux x $E^{2.7}$ vs kinetic energy per nucleon [8.4 GeV- 3.8 TeV]

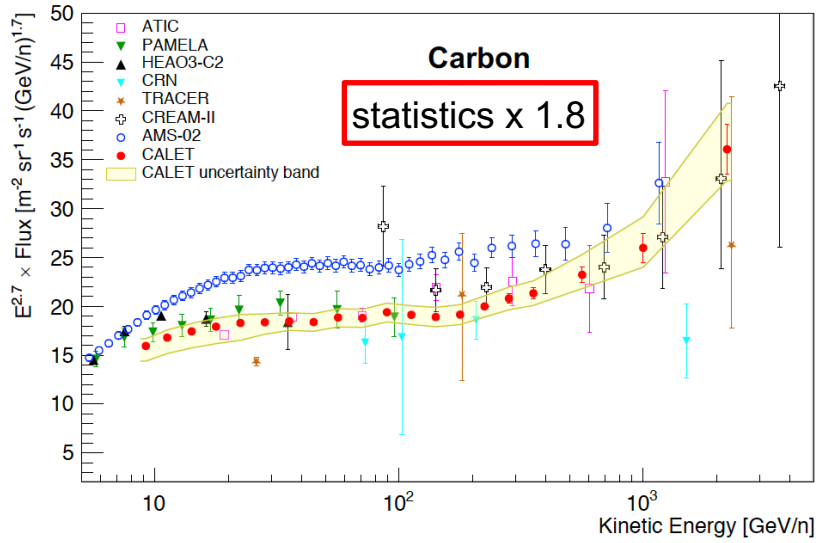

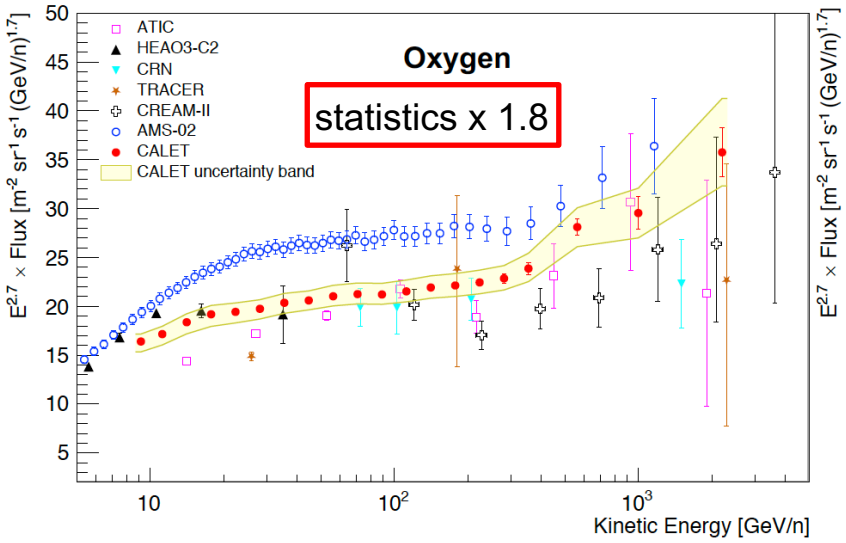

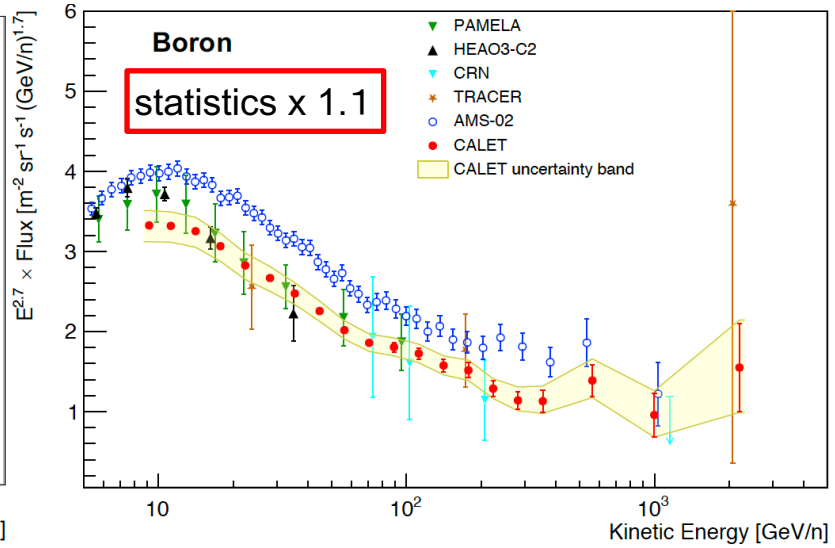

Fitting with double power law function

$$\Phi(E) = \begin{cases} c\left(\frac{E}{\mathrm{GeV}}\right)^{\gamma} & E \le E_0 \\ c\left(\frac{E}{\mathrm{GeV}}\right)^{\gamma}\left(\frac{E}{E_0}\right)^{\Delta\gamma} & E > E_0 \end{cases}$$

C-O fit
$\gamma = -2.66 \pm 0.02$
$E_0 = (260 \pm 50)$ GeV/n
$\Delta\gamma = 0.19 \pm 0.04$
χ^2/dof = 23/25

B fit
$\gamma = -3.03 \pm 0.03$
E_0 fixed from C-O
$\Delta\gamma = 0.32 \pm 0.14$
χ^2/dof = 5.2/11

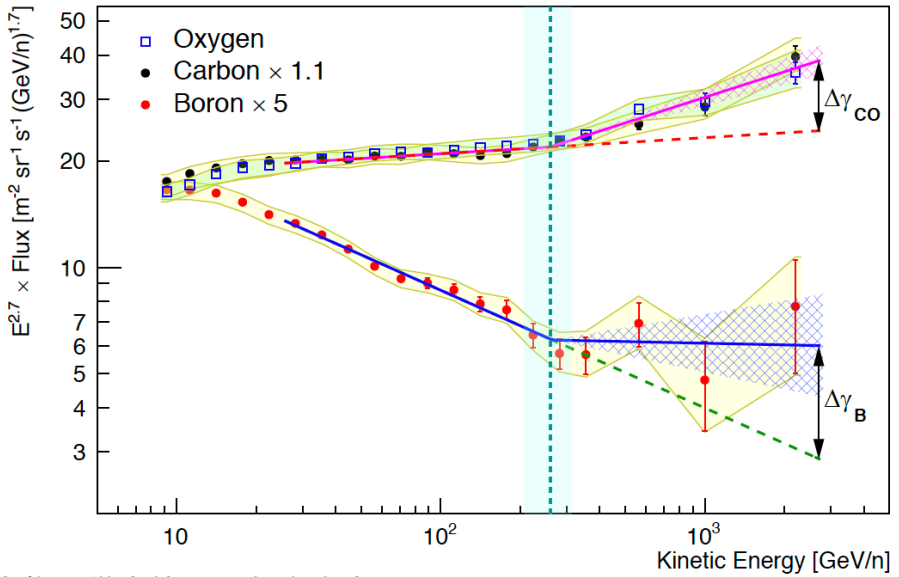

- C and O fluxes harden in a similar way above 200 GeV/n.
- B spectrum clearly different from C-O as expected for primary and secondary CR.
- The flux hardens more for B than for C and O above 200 GeV/n, albeit with low statistical significance.

B/C, B/O and C/O Flux Ratio

B/C flux ratio

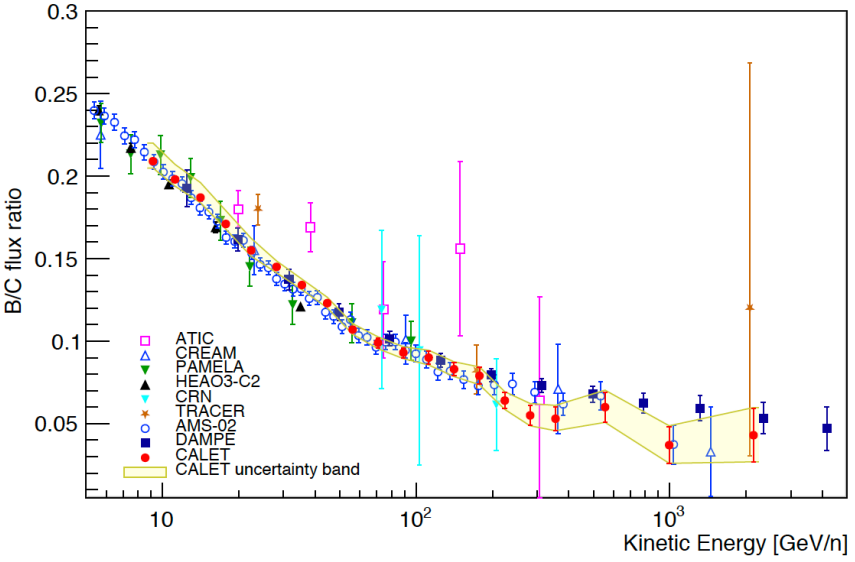

B/O flux ratio

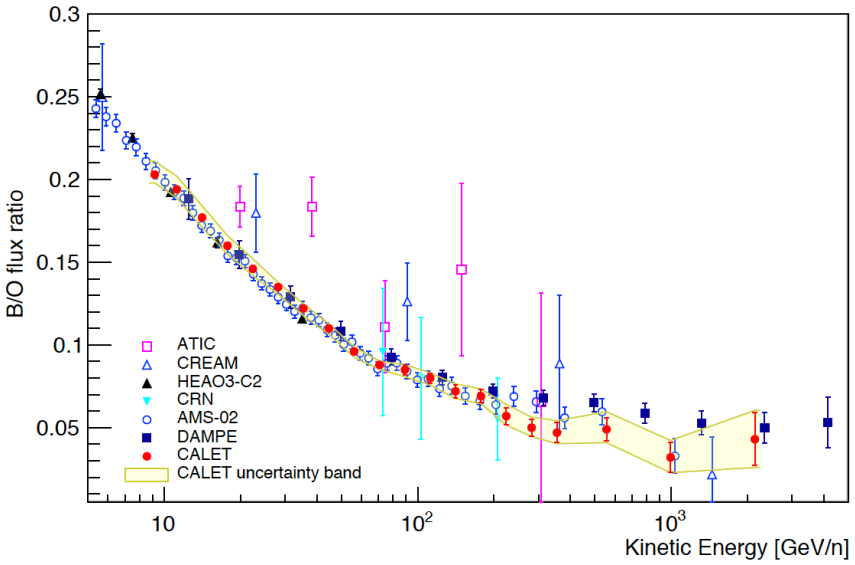

C/O flux ratio

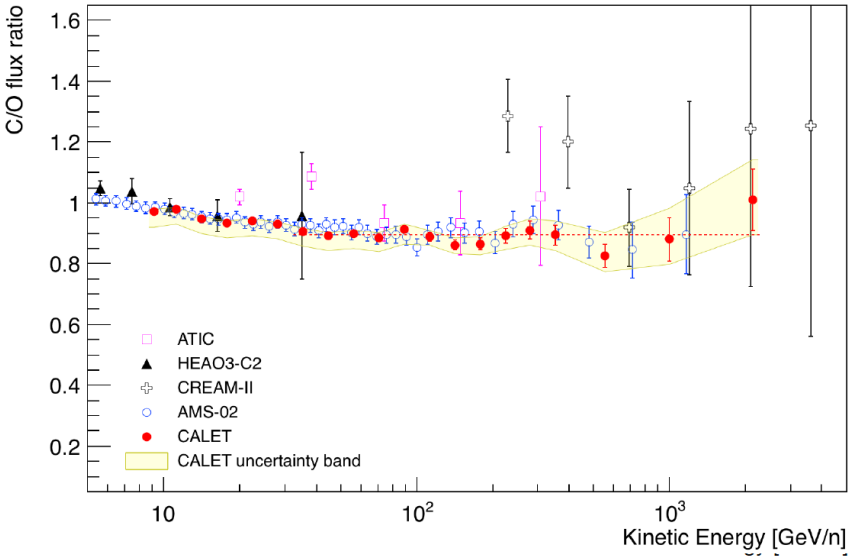

- Flux ratios of B/C and B/O are in agreement with AMS02 and lower than DAMPE result above 300 GeV/n, although consistent within the error bars.
- C/O flux ratio as a function of energy is in good agreement with AMS-02.
- At E > 30 GeV/n the C/O ratio is well fitted to a constant value 0.90 ± 0.03 with $\chi^2/\mathrm{dof} = 8.1/13$.
  ⇨ C and O fluxes have the same energy dependence.
- At E < 30 GeV/n C/O ratio is slightly softer.
  ⇨ secondary C from O and heavier nuclei spallation

Spectral Fit of B/C and B/O

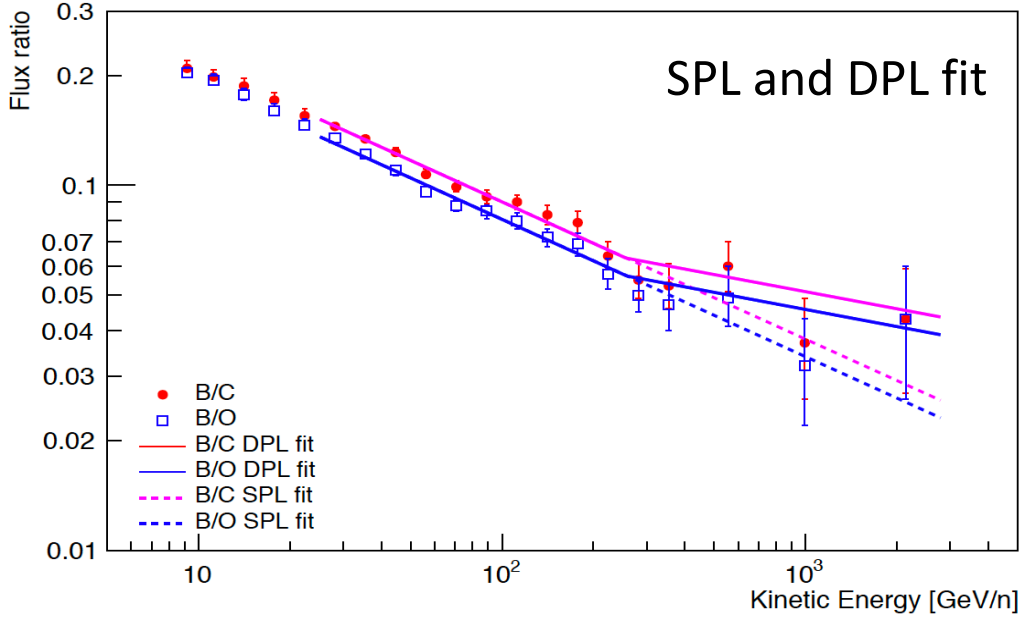

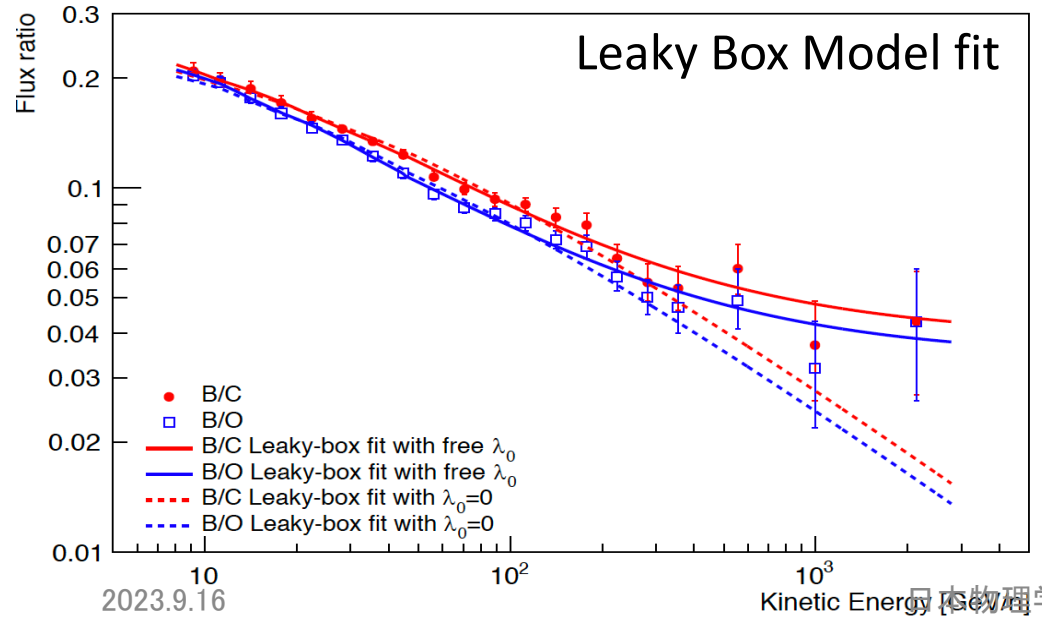

Simultaneous fit to B/C and B/O (E>25 GeV/n) with same parameters except normalization

SPL fit	$\Gamma = -0.376 \pm 0.014$	(χ^2/dof = 19/27)
DPL fit	$\Delta\Gamma = 0.22 \pm 0.10$	(χ^2/dof = 15/26)

Leaky-box model fit [ApJ **752** 69 (2012)]

$$\frac{\Phi_B(E)}{\Phi_C(E)} = \frac{\lambda(E)\lambda_B}{\lambda(E)+\lambda_B}\left[\frac{1}{\lambda_{C\to B}} + \frac{\Phi_O(E)}{\Phi_C(E)}\frac{1}{\lambda_{O\to B}}\right] \quad \frac{\Phi_B(E)}{\Phi_O(E)} = \frac{\lambda(E)\lambda_B}{\lambda(E)+\lambda_B}\left[\frac{1}{\lambda_{O\to B}} + \frac{\Phi_C(E)}{\Phi_O(E)}\frac{1}{\lambda_{C\to B}}\right]$$

$\lambda(E)$: mean escape path length

$\lambda(E) = kE^{-\delta} + \lambda_0$

λ_0 : residual path length

δ : diffusion coefficient spectral index

See details of assumption in CRD4-04 by Paolo Maestro

Fit parameters	λ_0 =0 fixed	λ_0 free
k (g/cm^2)	13.1 ± 0.2	13.0 ± 0.3
δ	0.61 ± 0.01	0.81 ± 0.04
λ_0 (g/cm^2)	0	1.17 ± 0.16
χ^2/dof	58.3/38	17.9/37

Significance of $\lambda_0 \neq 0 > 5\sigma$ ⇨ Residual path length could explain the flattening of B/C, B/O ratios at high energies.

Flux Ratio between Light Nuclei Primary Elements

C/He and O/He ratio with constant fitting

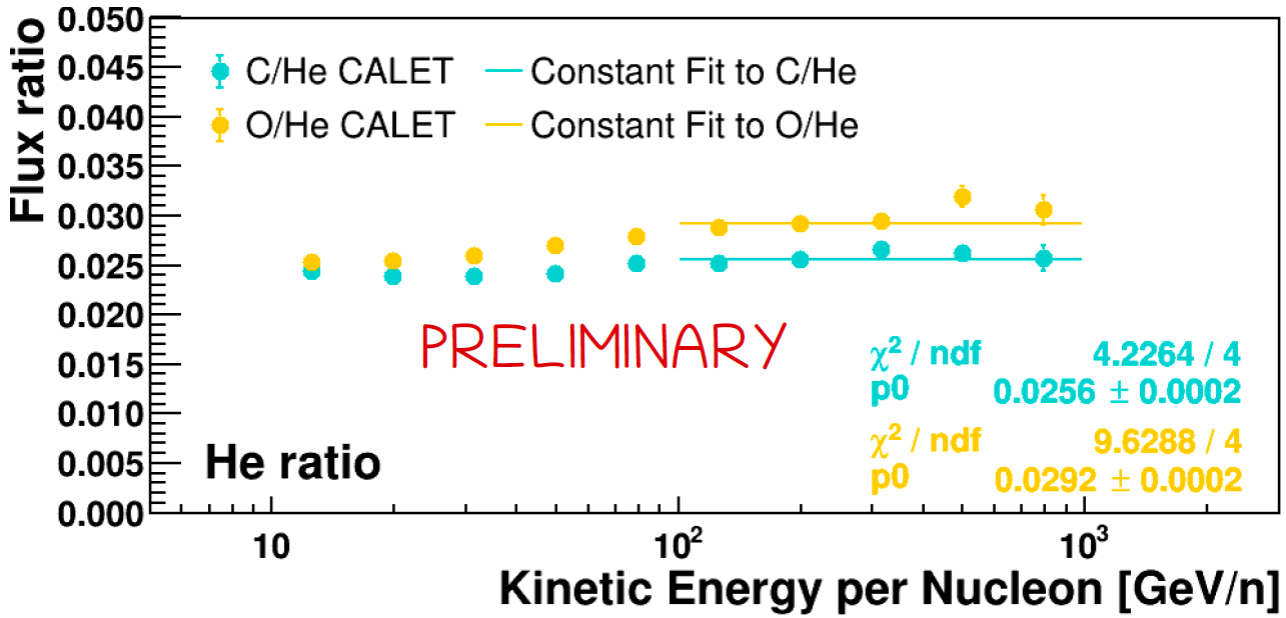

O/C ratio with constant fitting

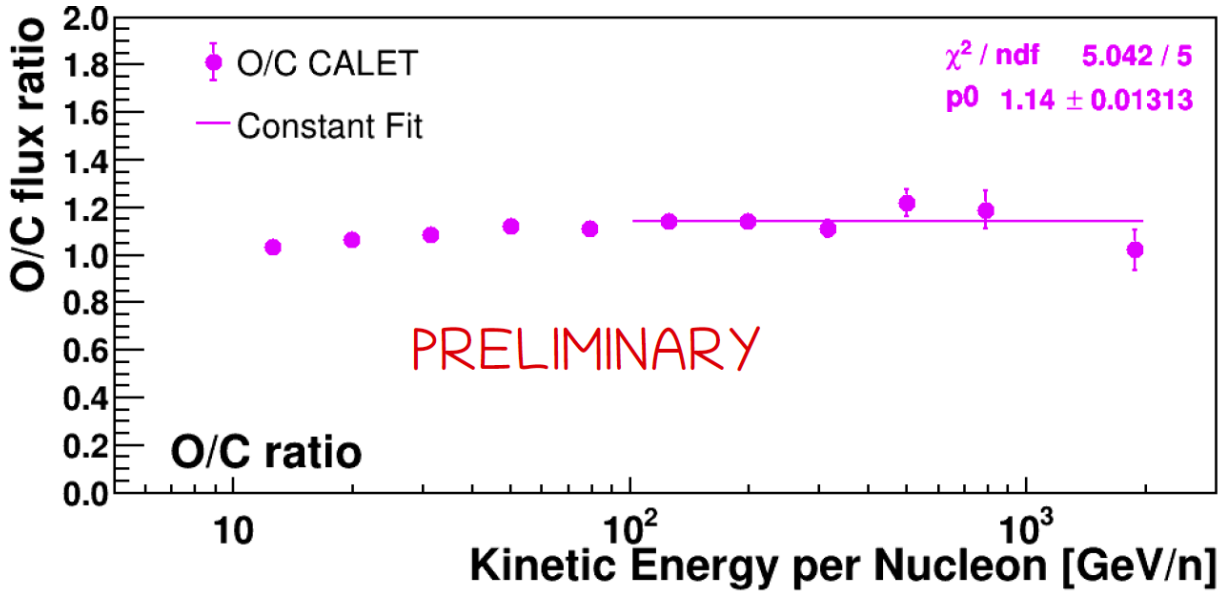

The flux ratio between light nuclei (He, C, O) is constant above 100 GeV/n.

Iron Energy Spectrum

Flux x $E^{2.6}$ vs kinetic energy per nucleon (Nov.2016-Dec.2022)

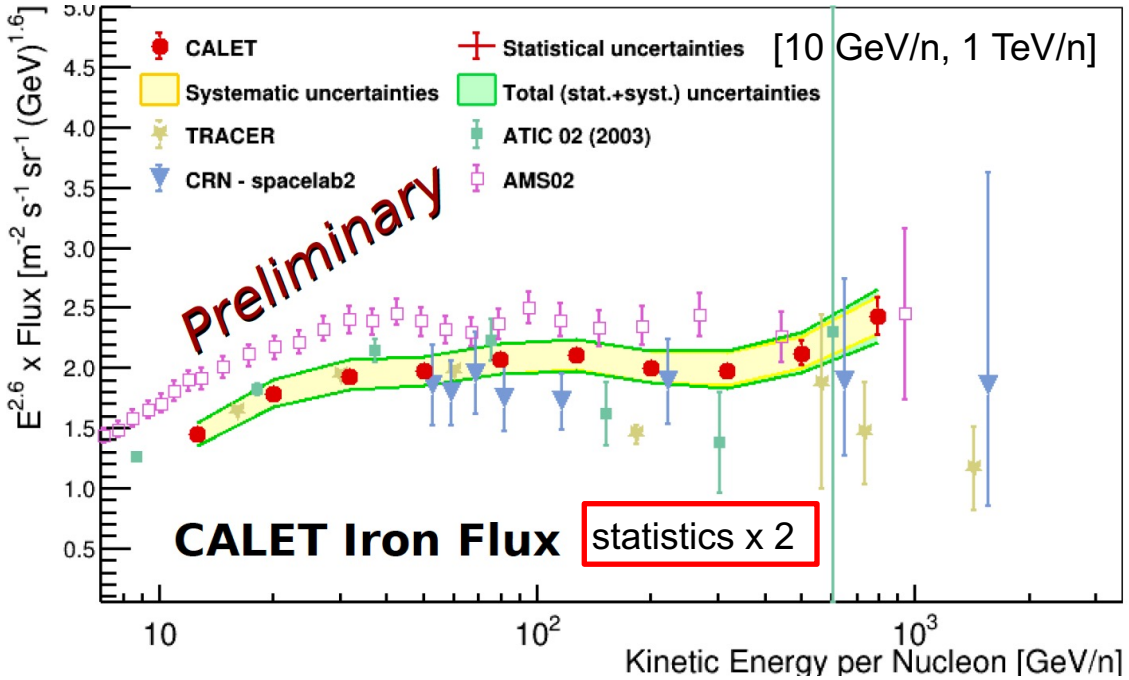

Fit from 50 to 800 GeV/n, with SPL & DPL

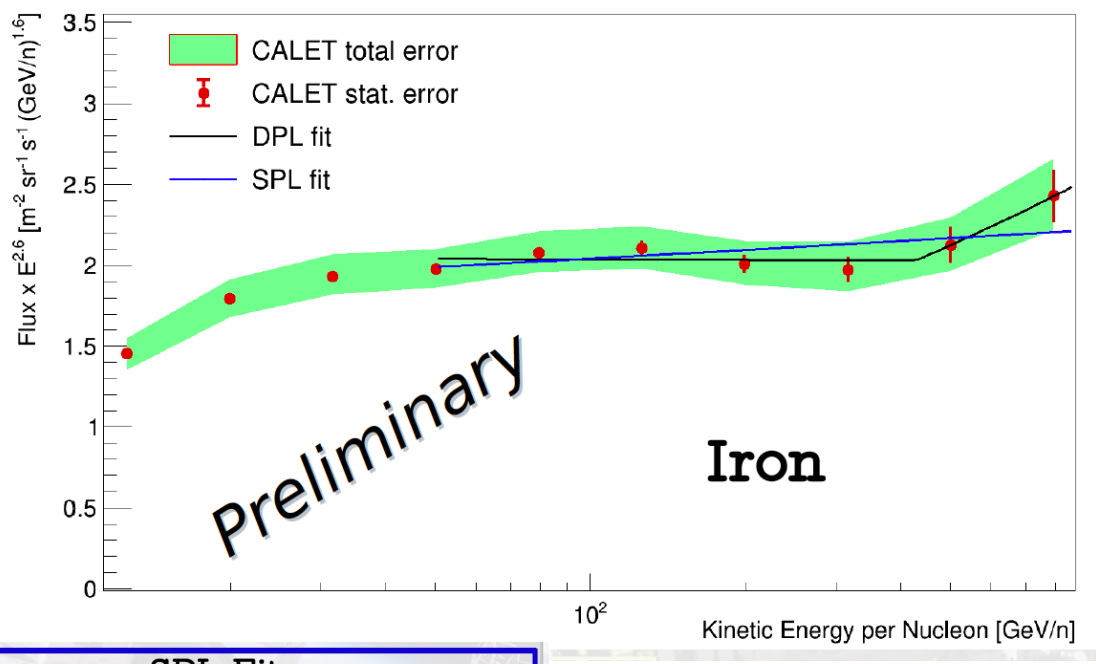

Low energy (< 10 GeV) measurement using geomagnetic cut-off (Oct. 2015 to May 2021)

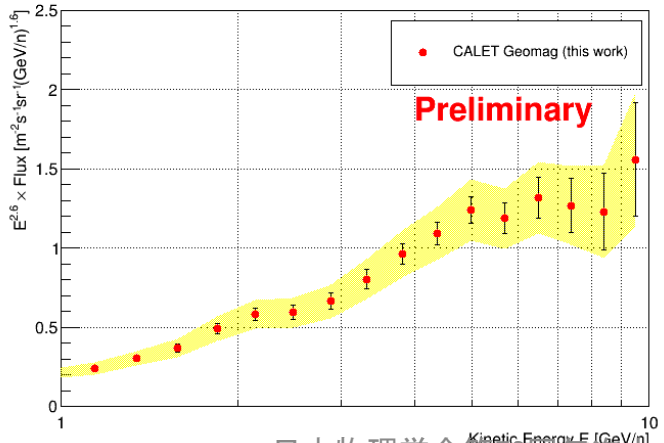

SPL Fit

$$\Phi(E) = C\left(\frac{E}{1\ \mathrm{GeV}}\right)^{\gamma}$$

- $\gamma = -2.56 \pm 0.01(\mathrm{stat}) \pm 0.03(\mathrm{sys})$
- $\chi^2/\mathrm{DOF} = 2.7/5$

DPL Fit

$$\Phi(E) = \begin{cases} c\left(\frac{E}{\mathrm{GeV}}\right)^{\gamma} & E \le E_0 \\ c\left(\frac{E}{\mathrm{GeV}}\right)^{\gamma}\left(\frac{E}{E_0}\right)^{\Delta\gamma} & E > E_0 \end{cases}$$

- $\gamma = -2.60 \pm 0.01(\mathrm{stat}) \pm 0.08(\mathrm{sys})$
- $\chi^2/\mathrm{DOF} = 0.8/3$
- $\Delta\gamma = 0.29 \pm 0.27$
- $E_0 = (428 \pm 314)$ Gev/n

The significance of the fit with the DPL in the studied energy range is not sufficient to exclude the possibility of a single power law

Flux Ratios of Iron to Primary Elements

Fe ratios to He, C and O

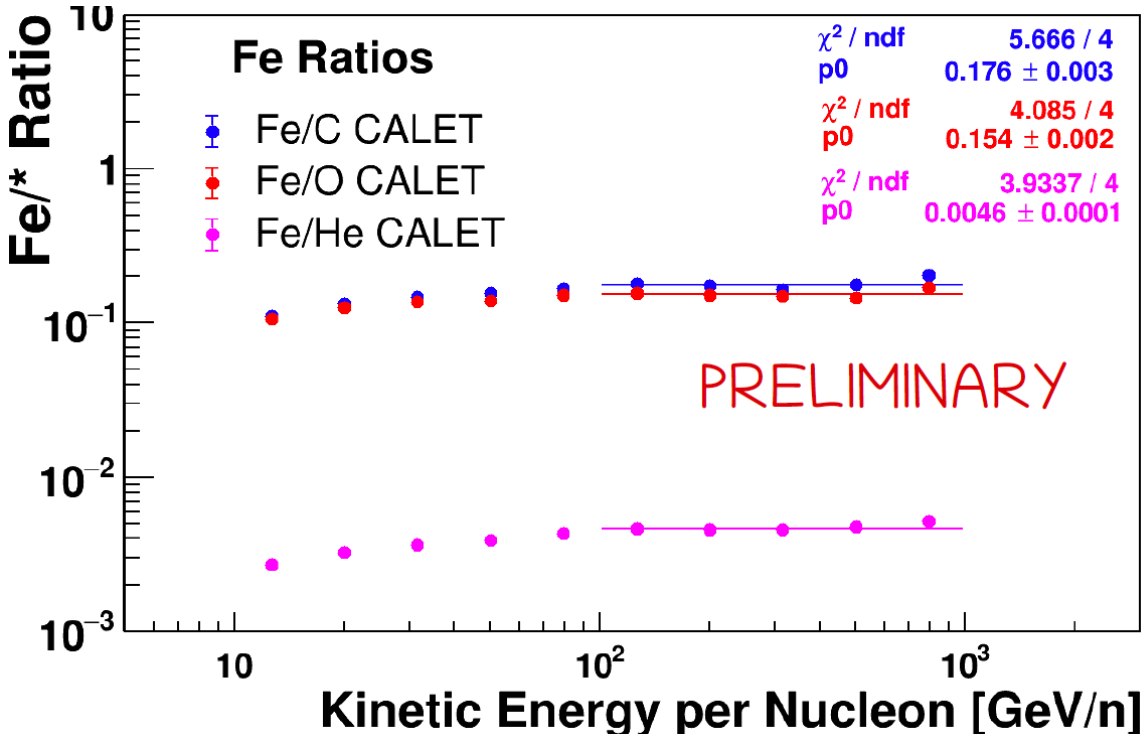

Fe ratios to He, C and O normalized at 100 GeV/n

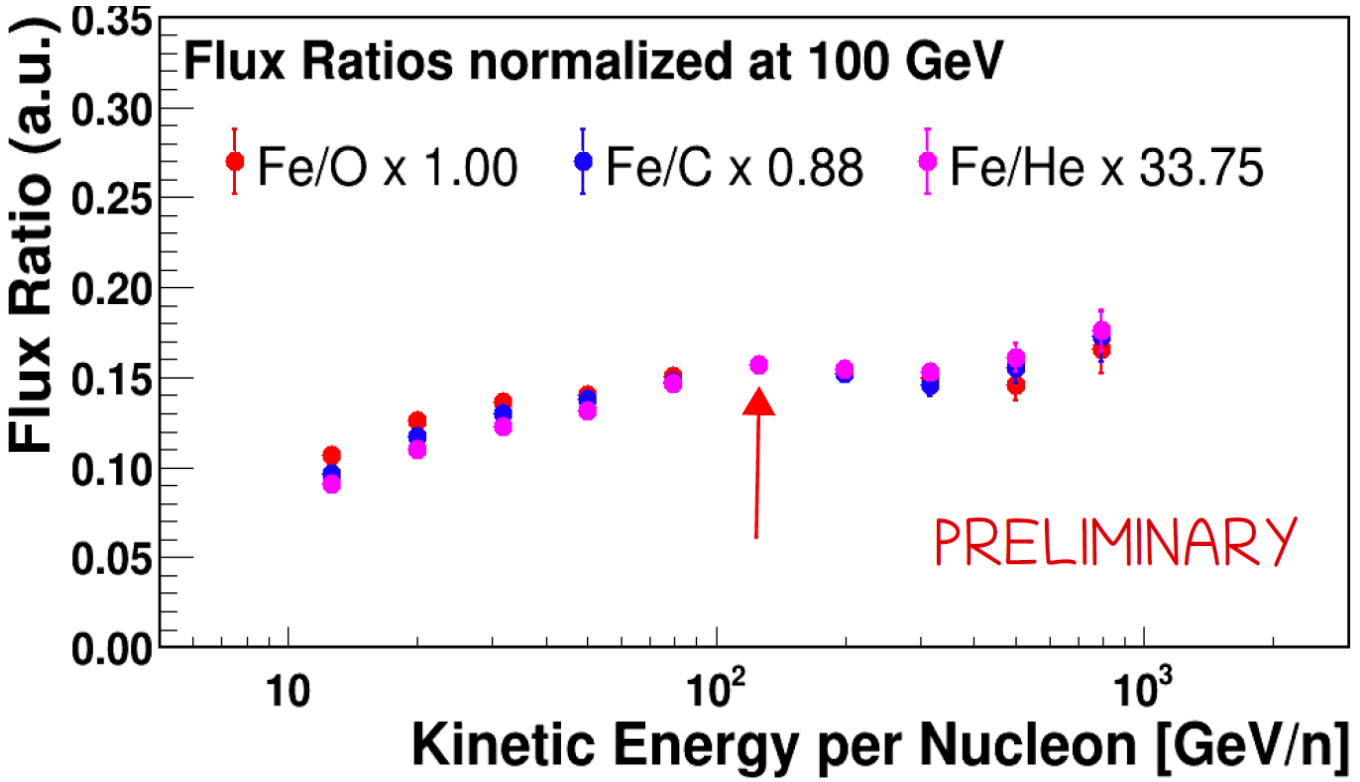

Fe/O, Fe/C and Fe/He are compatible with a constant above 100 GeV/n within errors.
⇨ Fe, O, C follow similar propagation

Nickel Energy Spectrum

Flux x $E^{2.6}$ vs kinetic energy per nucleon

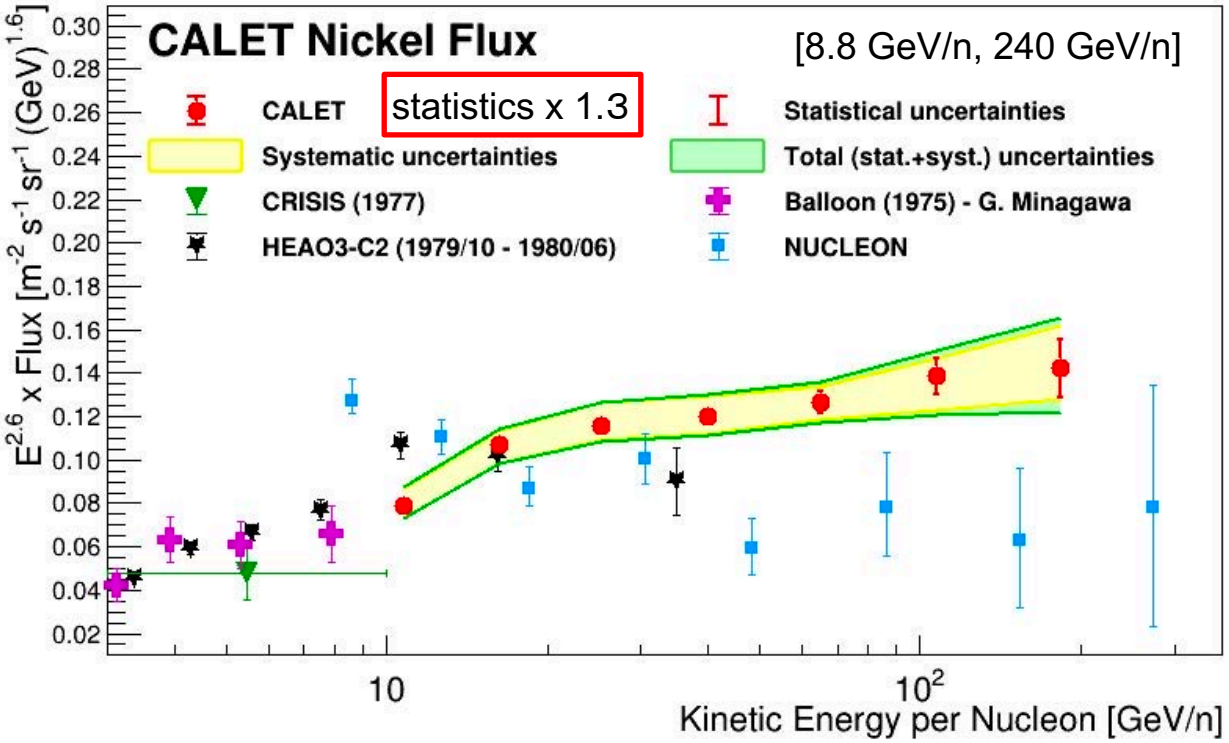

Fit from 20 to 240 GeV/n, with a SPL

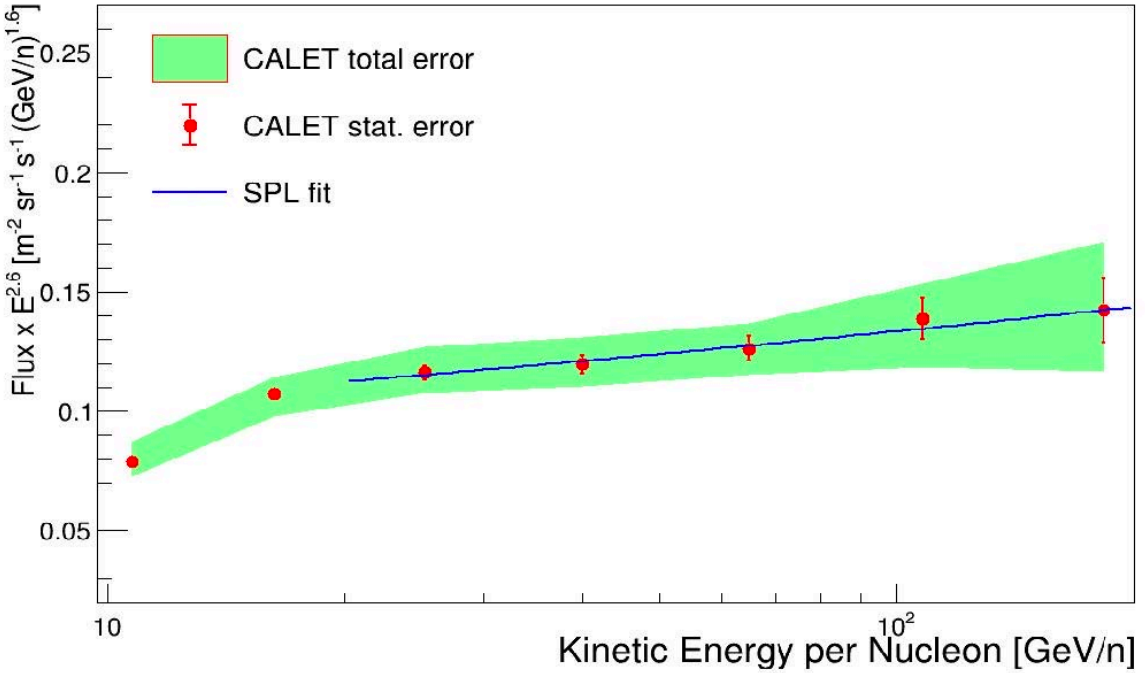

Charge separation between Fe and Ni

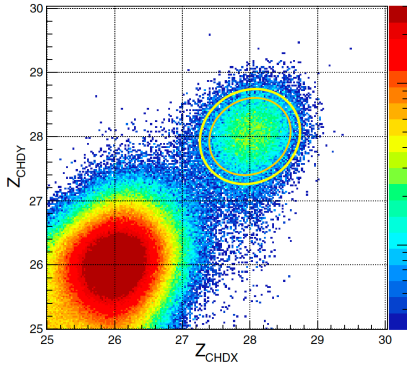

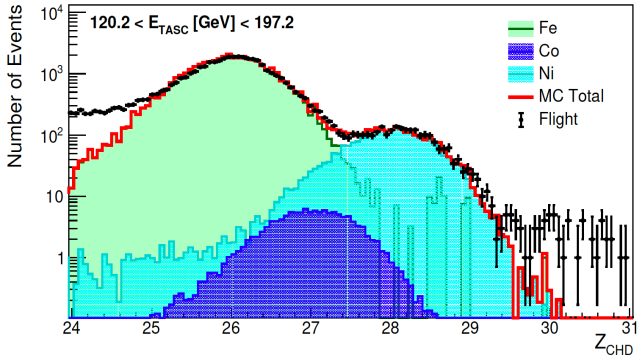

SPL Fit

$$\Phi(E) = C\left(\frac{E}{1\ \mathrm{GeV}}\right)^{\gamma}$$

- $\gamma = -2.49 \pm 0.03(\mathrm{stat}) \pm 0.07(\mathrm{sys})$
- $\chi^2/\mathrm{DOF} = 0.1/3$

From 20 to 240 GeV/n the nickel flux is consistent with the hypothesis of an SPL Spectrum.

Flux Ratios of Nickel to Primary Elements

Ni ratios to He, C, O and Fe

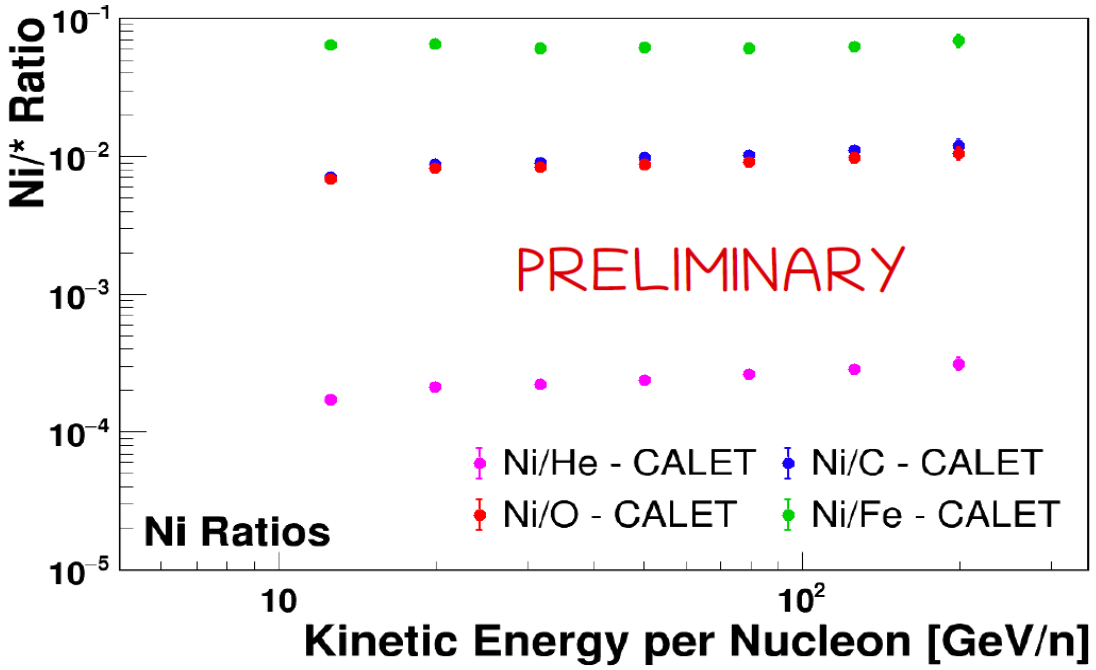

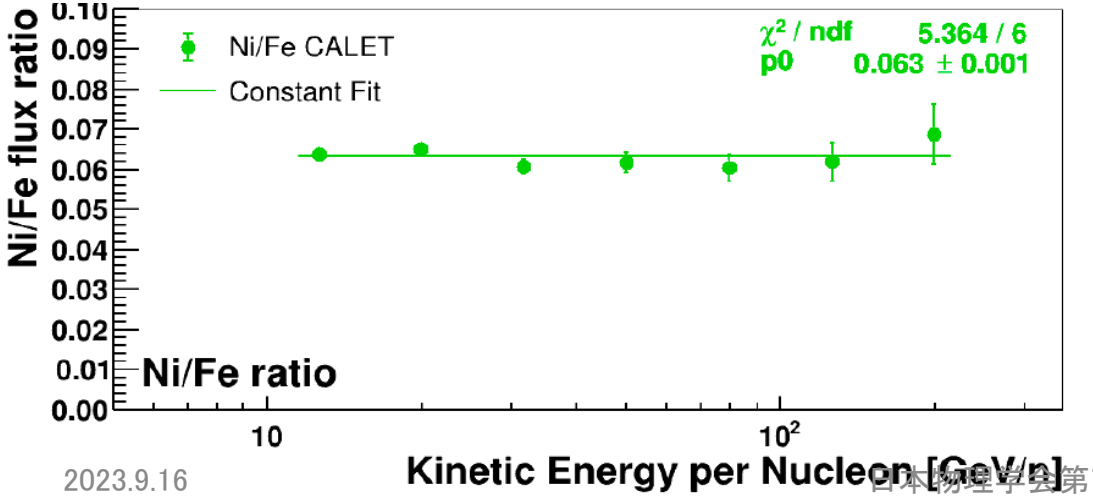

Ni ratios normalized at around 10 GeV/n

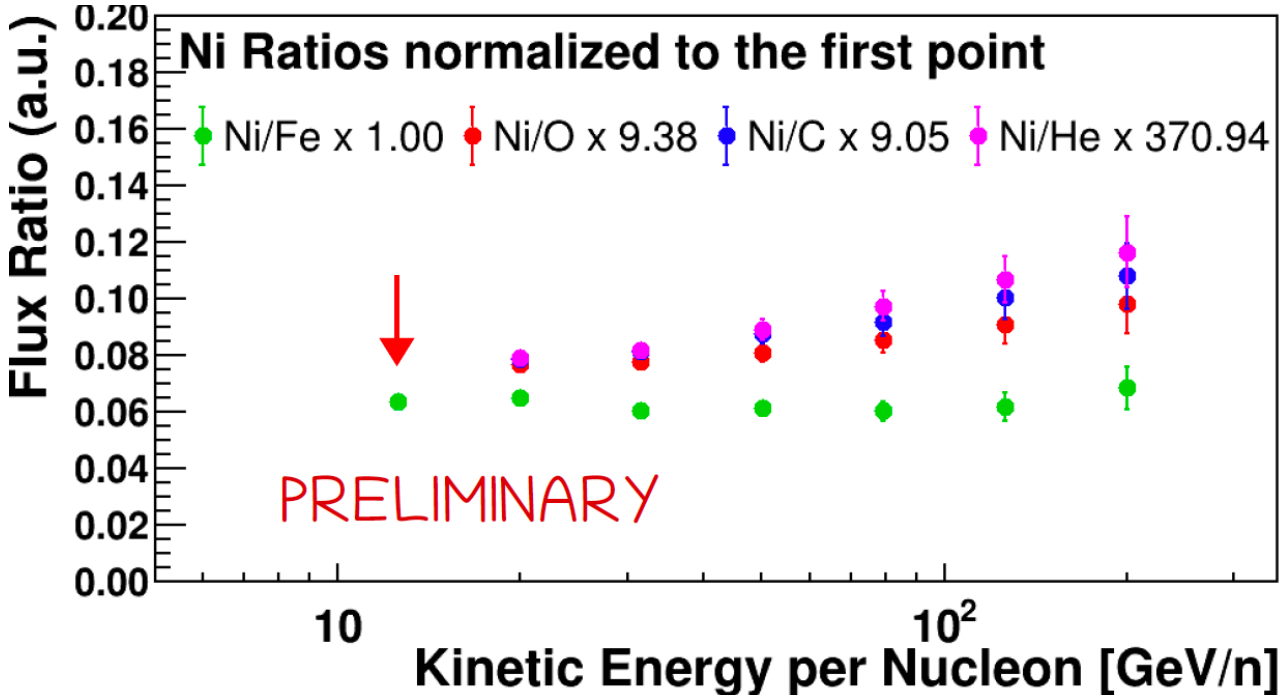

- The Ni/Fe flux ratio is constant in all the energy range thus Ni and Fe have very similar behavior.
- The present energy range of nickel flux does not allow to fit the Ni/* ratios with a constant above 100 GeV/n.
- At low energy the Ni/O, Ni/C, Ni/He flux ratio show an increasing trend also visible in Fe/* ratios.

Ultra-heavy Cosmic-ray Nuclei (26 < Z ≤ 44)

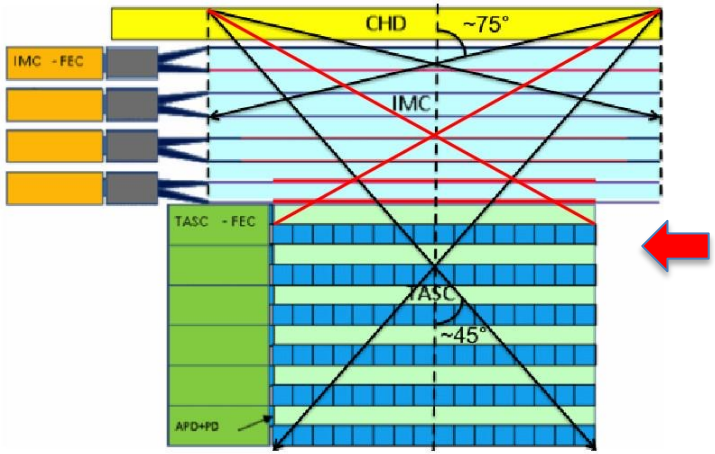

- A special UH CR trigger uses the CHD and the first 4 layers of the IMC to achieve an expanded x 4 geometric factor **GF ~ 4400 cm^2 sr** without energy information.
  (~260 million events)
- A subset of events pass through the top of the TASC (~65 million events) with energy information,

Charge histogram

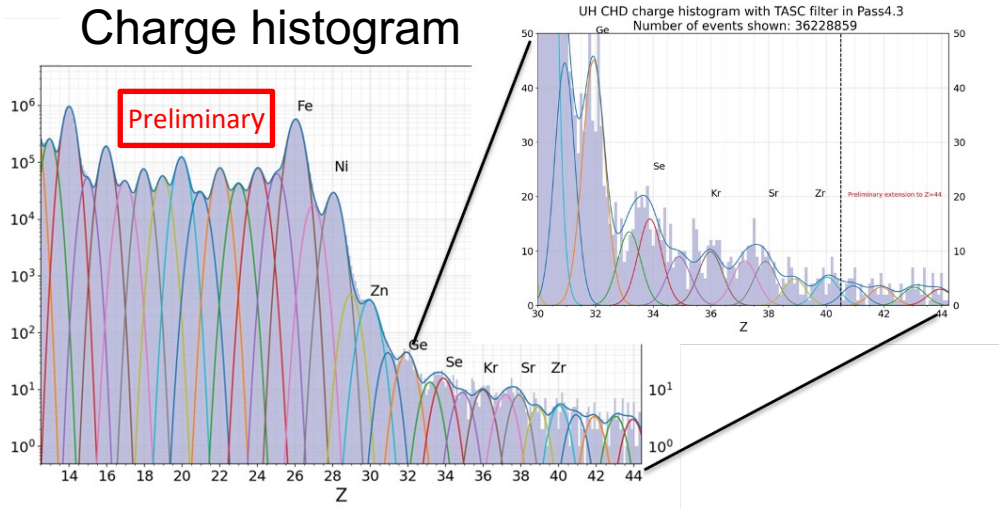

Mesurement of the relative abundances of the elements above Fe through $_{44}$Ru (Fe =1)

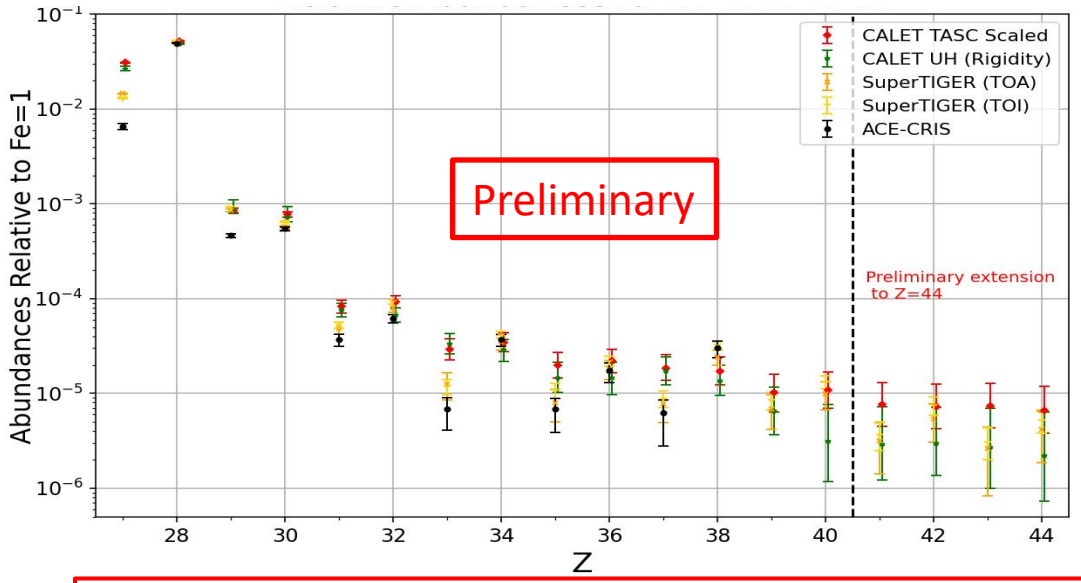

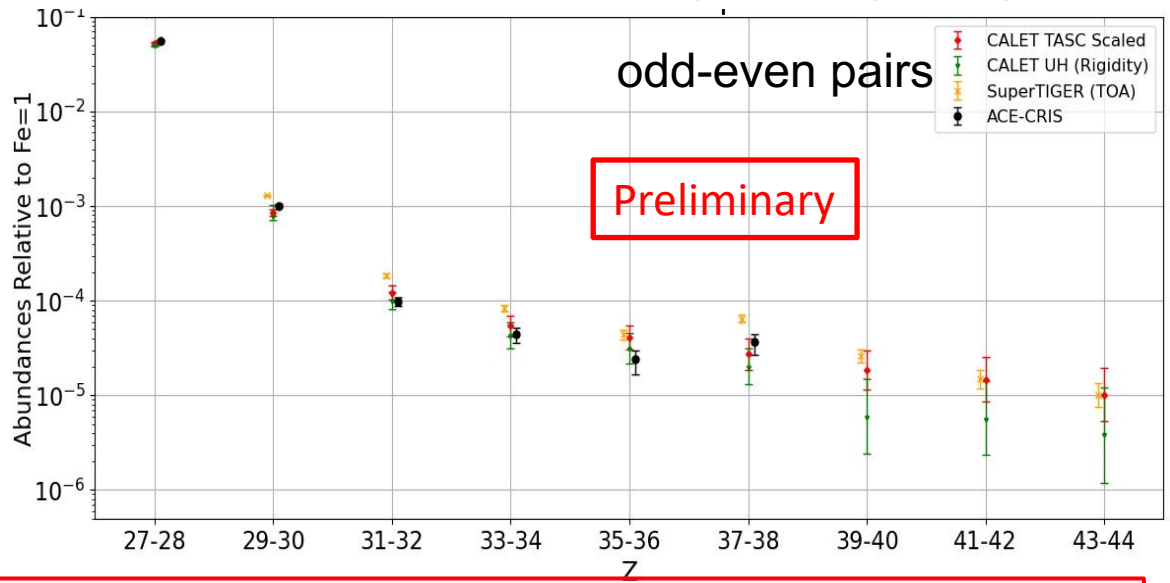

The CALET UH element ratios relative to Fe are consistent with Super-TIGER and ACE abundances.

Summary and Future Prospects

CALET was successfully launched in August 2015 and installed on the JEM-EF module on the ISS

- Operational over 2800 days with 86% live time, total triggers approaching 4 billion
  - Continuous on-orbit updates from ground calibration — Astropart. Phys. 91, 1 – 10 (2017)
  - Stable operations over a range of observing modes continue — Astropart. Phys. 100, 29 – 37 (2018)
- Analysis of CR events continues, extending to higher energies and charges

All-electron spectrum in the range 11 GeV – 4.8 TeV	PRL 120, 261102 (2018)	(2nd update)
Proton spectrum in the range 50 GeV – 60 TeV	PRL 129, 101102 (2022)	(2nd update)
Carbon and oxygen spectra in the range 10 GeV/n – 2.2 TeV/n	PRL 125, 251102 (2020)	1st paper
Iron spectrum in the range 50 GeV/n – 2 TeV/n	PRL 126, 241101 (2021)	1st paper
Nickel spectrum in the range 8.8 GeV/n – 240 GeV/n	PRL 128, 131103 (2022)	1st paper
Boron spectrum in the range 8.4 GeV/n – 3.8 TeV/n	PRL 129, 251103 (2022)	new
Helium spectrum in the range 40 GeV – 250 TeV	PRL 130, 171002 (2023)	new
Preliminary analysis of ultra-heavy cosmic-ray abundances	see W.Zober CRD3-06 (ICRC2023)	preliminary

- Analysis of gamma-ray sources and transients continues
  - Calorimeter instrument response characterized — ApJS 238:5 (2018)
  - GW follow-up and GRB analysis with CGBM & CAL — ApJL 829:L20 (2016)
  - Counterpart search in LIGO/Virgo O3 with CGBM & CAL — ApJ 933:85 (2022)
- Analysis of transient heliospheric and space weather phenomena underway

Charge-sign dependence of Solar modulation	PRL 130, 211001 (2023)	new

Extended operations approved by JAXA/NASA/ASI in March 2021 through the end of 2024 (at least)

✓ We greatly appreciate JAXA staffs for perfect support of the CALET operation at the TKSC of JAXA !!

✓ **This work is partially supported by JSPS KAKENHI Kiban (S) Grant Number 19H05608 (2019-2023FY)**